ULTRASOUND-ASSISTED EXTRACTION OF XANTHONE FROM MANGOSTEEN PERICARP USING A MIXTURE OF VIRGIN COCONUT OIL AND ETHANOL

By

YAO ZHENGYUAN

Thesis Submitted to the School of Graduate Studies, Universiti Putra Malaysia, in Fulfilment of the Requirements for the Degree of Master of Science

September 2024

FSTM 2024 17

Abstract of thesis presented to the Senate of Universiti Putra Malaysia in fulfilment of the requirement for the degree of Master of Science

ULTRASOUND-ASSISTED EXTRACTION OF XANTHONE FROM MANGOSTEEN PERICARP USING A MIXTURE OF VIRGIN COCONUT OIL AND ETHANOL

By

YAO ZHENGYUAN

September 2024

Chairman : Chong Gun Hean, PhD
Faculty : Food Science and Technology

As an organic ingredient contained in mangosteen pericarp (MP), xanthone is more and more widely used in functional food, cosmetics and pharmaceuticals because it shows a variety of potential medical values. However, the existing extraction process of xanthone from MP still needs to be improved, especially the choice of extraction method and solvent type. The aim of this study was to improve the extraction yield of xanthone from mangosteen pericarp using ultrasound-assisted extraction (UAE) with appropriate parameters in a binary solvent mixture of ethanol and virgin coconut oil (VCO). The solubilities of xanthone in mixture of ethanol- VCO were measured at four temperatures (303.15 K- 323.15 K) using eleven volume ratios of ethanol and VCO (0:1-1:0). The concentration of xanthone was measured with spectrophotometer at 347 nm. The solubility test results showed that the solubility of xanthone in mixed-solvent was higher than pure ethanol and VCO. When the volume fraction of VCO increased to 0.6 and the temperature was 323.15 K, the

solubility reached the maximum value of 0.0329 g/g. The mixed-solvent, VCO (0.6): ethanol (0.4) was used in UAE of xanthone from MP, the intensities of ultrasound were controlled in 0 W- 25 W, and concentrations of xanthone were measured over time. With the UAE, the concentration of xanthone in the extract increased to up to 12%. The concentration of xanthone also increased linearly with the intensity of ultrasound and the extraction time. Peleg's model, pseudo-second order kinetic model type 2 and Respond Surface Method model can be used to predict the kinetics of UAE in extracting xanthone. The mixed-solvent approach in this study has demonstrated advantages over pure solvent and offered a more efficient option for xanthone extraction.

Keywords: xanthone, solubility, binary solvent, ultrasound assisted extraction, kinetic model

SDG: GOAL 4: Good Health and Well-Being, GOAL 9: Industry, Innovation and Infrastructure, GOAL 13: Climate Action.

Abstrak tesis yang dikemukakan kepada Senat Universiti Putra Malaysia sebagai memenuhi keperluan untuk ijazah Master Sains

EKSTRAKSI BERBANTU ULTRABUNYI DARIPADA XANTHONE DARI MANGOSTEEN PERICARP MENGGUNAKAN CAMPURAN MINYAK KELAPA DARA DAN ETANOL

Oleh

YAO ZHENGYUAN

September 2024

Pengerusi : Chong Gun Hean, PhD
Fakulti : Sains dan Teknologi Makanan

Sebagai bahan organik yang terkandung dalam kulit manggis, xanthone semakin banyak digunakan dalam makanan fungsian, kosmetik dan farmaseutikal kerana ia menunjukkan pelbagai nilai perubatan yang berpotensi. Namun, proses pengekstrakan xanthone sedia ada daripada perikarp manggis masih perlu dipertingkatkan terutamanya pemilihan kaedah pengekstrakan dan jenis pelarut. Matlamat kajian ini adalah untuk meningkatkan hasil pengekstrakan xanthone daripada kulit manggis dengan menggunakan pengekstrakan bantuan ultrabunyi (UAE) dan parameter yang sesuai dalam campuran pelarut binari etanol dan minyak kelapa dara (VCO). Keterlarutan xanthone dalam campuran etanol-VCO diukur pada empat suhu (303.15 K- 323.15 K) menggunakan sebelas nisbah isipadu etanol dan VCO (0:1- 1:0). Kepekatan xanthone diukur dengan spektrofotometer pada 347 nm. Keputusan ujian keterlarutan menunjukkan bahawa keterlarutan xanthone dalam pelarut campuran adalah lebih tinggi daripada etanol tulen dan VCO.

Apabila pecahan isipadu VCO meningkat kepada 0.6 dan 323.15 K, keterlarutan mencapai nilai maksimum iaitu 0.0329 g/g. Pelarut campuran, VCO (0.6): etanol (0.4), telah digunakan di pengektrakan xanthone UAE daripada MP, keamatan ultrabunyi dikawal dalam 0 W- 25 W, dan kepekatan xanthone diukur dari masa ke semasa. Dengan UAE, kepekatan xanthone dalam ekstrak meningkat sehingga 12%. Kepekatan xanthone juga meningkat secara linear dengan keamatan ultrabunyi dan masa pengekstrakan. Model Peleg, model kinetik tertib pseudo-kedua jenis 2 dan model *Respond Surface Method* boleh digunakan untuk meramalkan kinetik UAE dalam pengektrakan xantone. Pendekatan pelarut campuran dalam kajian ini telah menunjukkan kelebihan berbanding pelarut tulen dan menawarkan pilihan yang lebih efisien untuk pengekstrakan xanthone

Kata Kunci: Xanthone, Keterlarutan, Pelarut binari, Pengekstrakan dibantu ultrabunyi, Model kinetic

SDG: MATLAMAT 4: Kualiti Pendidikan, MATLAMAT 9: Industri, Inovasi Dan Infrastruktur, MATLAMAT 13: Tindakan Iklim

ACKNOWLEDGEMENTS

First and foremost, I would like to express my sincerest thanks to my supervisor Assoc. Prof. Dr. Chong Gun Hean for his patient guidance and professional assistance. His wisdom and knowledge led me to complete my research, and also passed on to me his spirit of continuous exploration of science.

I would also like to thank all members of my committee, Dr. Ismail Fitry Bin Mohammad Rashedi, and Professor. Wang Xinsheng for their various suggestions on the details of my research and suggestions for improvement.

Also, I am very grateful to all the staffs from Supercritical Fluid Centre (SFC), teaching laboratory and research laboratory of Faculty of Food Science and Technology (FSTM) of Universiti Putra Malaysia (UPM) as well as staffs from Henan University of Science and Technology for providing kind advises and assistance in this project.

I also wish to thank my parents for their understanding, their support of my studies has lessened the obstacles in my master journey. In addition, I would also like to thank the classmates and laboratory members who studied with me for their encouragement and assistance.

Nevertheless, I would like to thank the companies that provided plant materials, chemical reagents, and instruments for this study. Their reliable products provided the conditions for the success of my research.

This thesis was submitted to the Senate of Universiti Putra Malaysia and has been accepted as fulfilment of the requirement for the degree of Master of Science. The members of the Supervisory Committee were as follows:

Chong Gun Hean, PhD
Professor
Faculty of Food Science and Technology
Universiti Putra Malaysia
(Chairman)

Ismail Fitry bin Mohammad Rashedi, PhD
Professor
Faculty of Food Science and Technology
Universiti Putra Malaysia
(Member)

Wang Xinsheng, PhD
Associate Professor
School of Chemistry & Chemical Engineering
Henan University of Science and Technology,
China
(Member)

ZALILAH MOHD SHARIFF, PhD
Professor and Dean
School of Graduate Studies
Universiti Putra Malaysia

Date:

TABLE OF CONTENTS

LIST OF TABLES

LIST OF FIGURES

LIST OF ABBREVIATIONS

MP	Mangosteen pericarp
K	Kelvin
$scCO_2$	Supercritical carbon dioxide
VCO	Virgin coconut oil
CKD	Chronic kidney disease
UAE	Ultrasound-assisted extraction
MCTs	Medium-chain triglycerides
HSP	Hansen solubility parameter
MAE	Microwave-assisted extraction
AMBS	Aqueous micellar biphasic system
RSM	Response surface methodology
HPLC	High-Performance Liquid Chromatography

CHAPTER 1

INTRODUCTION

1.1 Background

Mangosteen (*Manggis* in Malay) is a widely distributed fruit in tropical regions, especially in Asia. In Southeast Asia, mangosteen commonly known as the “Queen of Fruits”, is consumed directly as a fresh fruit. However, due to its seasonality, the market cycle of fresh mangosteen is only 6 weeks to 10 weeks. Therefore, to meet market demand, mangosteen has been processed into various products, including syrup, canned fruit, dried forms, and others. Consequently, a significant amount of inedible parts such as seeds and mangosteen pericarp (MP) are produced in the process (Kok et al. 2021). The agricultural statistics department of Malaysia monitored the mangosteen industry data and found that the output of discarded MP nationwide accounts for about 60% of the weight of the raw material fruit. For this fruit that has received widespread attention, Malaysia’ s estimated mangosteen production in 2010 was 29,520 tons, of which MP production was 17,712 tons (Nasrullah et al. 2019). In fact, the by-products contain a variety of bioactive components that could be recovered and converted into nutritional health products and functional foods.

As reported by previous studies, MP has shown efficacy in treating chronic ulcers, stomach pains, diarrhea, and certain skin conditions (Vargas-Campos et al. 2023). Most of the bioactive ingredients found in MP are xanthone derivatives, classified as polyphenolic compounds. Xanthone was an organic

compound with similar molecular composition to the phenolic compounds contained in MP. The derivatives of xanthone in mangosteen, especially α-mangosteen and γ-mangosteen (Morini et al. 2020), have shown significant antioxidant activity, scavenging the free-radical species (Zheng et al. 2021), antibacterial activity, anti-diabetes efficacy and some beneficial medical properties such as antitumor, anticancer, neuroprotective, cytoprotective, antiulcer, antimalarial, antiacne, antiallergic, anti-inflammatory, and histamine receptor blocker (Phyo et al. 2021). These characteristics make the extract of MP more and more widely used in functional food, cosmetics, pharmaceutical and neutral food. The study of xanthone solubility was of great help to improve the extraction amount of phenolic active components in mangosteen peel and optimize the extraction steps (Kalick et al. 2023).

The conventional techniques, involving the use of a single solvent for recovering xanthones from mangosteen peel, include organic solvent extraction (Ethyl acetate, ethanol and hexane), hot water extraction, subcritical ethanol extraction, and supercritical carbon dioxide ($scCO_2$) extraction (Mohammad et al. 2019). However, employing a mixture of different solvents with distinct properties could yield synergistic effects (Qiu et al. 2019). Numerous studies have demonstrated that using a mixed-solvent approach is effective for enhancing drug solubility. For example, relationship between the molar fraction solubility of itraconazole at 298.15 K and the proportion of methyl chloride in a binary mixed solvent (Lee et al. 2023); the solubility of dodecanedioic acid in a mixed solvent of ethyl acetate and ethanol affected by the proportion of ethyl acetate (Cheng et al. 2022) and mole fraction solubility

of mesalazine in the aqueous mixtures of 2-propanol (Mazaher Haji Agha et al. 2020). Beyond improving solubility, a carefully chosen mixed-solvent can also mitigate certain drawbacks associated with a single solvent, such as challenging separation, slow extraction, and solvent toxicity (Yan et al. 2023). Li et al. used the optimized hexamethyldisiloxane, isoamyl acetate, ethyl acetate, and propylene carbonate liquid-liquid extraction mixed solvent in the isobutanol wastewater treatment industry, which reduced production costs and improved extraction efficiency (Li et al. 2024).

1.2 Objectives

The priority of this study is to explore the impact of ethanol as a co-solvent to virgin coconut oil (VCO) on the ultrasound-assisted extraction of xanthones from mangosteen pericarp. Specific objectives were:

1 To determine the solubility of xanthone in a mixture of VCO and ethanol across different temperatures.

2 To correlate solubility data with empirical models.

3 To compare the efficacy of the VCO and ethanol mixture with their respective pure solvents in ultrasound-assisted xanthone extraction from MP.

1.3 Scope and Significance of Study

This research focused on enhancing recovery of xanthone from mangosteen peel through the application of a mixed-solvent approach, using a combination of virgin coconut oil (VCO) + ethanol. The scope of the study addresses a critical gap in the understanding of the solubility behavior of xanthone within

the VCO-ethanol system, considering factors such as the solvent ratio, properties of the mixed-solvent, and varying temperatures. By elucidating these aspects, this study not only contributes to the scientific knowledge of xanthone extraction but also practical significance in efficient and sustainable extraction processes. With potential applications in industries seeking eco-friendly solutions for the recovery of valuable bioactive compounds from natural sources.

CHAPTER 2

LITERATURE REVIEW

2.1 Xanthone

In the realm of natural product chemistry, xanthone stands out as one of the most prevalent types of chemical species. These compounds are secondary metabolites produced by higher plant families, fungi, lichens, and bacteria, primarily found in Gentianaceae, Polygalaceae, Clusteraceae, and several other families. Xanthones exhibit a variety of health-promoting properties, such as antibacterial, anticancer, antioxidant, and antidiabetic effects. The chemical formula of xanthone is $C_{13}H_8O_2$. Its core structure is 9H-xanthen-9-one, featuring a dibenzo-γ-pyrone scaffold, which is often referred to as a "privileged structure" due to its significant biological activity. (Pinto et al. 2021), since its medical potential is affected by slight differences in structure among similar compounds. The classical planar molecular structure of xanthone in the conventional solid state is generally believed to be derived from its iconic conjugated ring. However, the oxygen atom deviates slightly from the plane by 0.13 Å. Additionally, the central pyran ring exhibits a partially aromatic character (Morini et al. 2020). Xanthone has been found to be a compound with strong chemical stability. The reason for this can be intuitively understood as its structural framework (tricyclic fused ring) is more rigid than chain compounds, making its structure difficult to change. The chemical derivatives of xanthone have a certain degree of difference, which is usually related to the different types and positions of substituents on the structural framework (Żelaszczyk et al. 2024). Xanthones can interact with various biological targets

due to several key molecular characteristics. These include a largely planar and rigid heteroaromatic tricyclic ring system, a central carbonyl group capable of multiple interactions, biaryl ether groups that contribute to the electron system, and a xanthone core that supports numerous substituents in various positions.

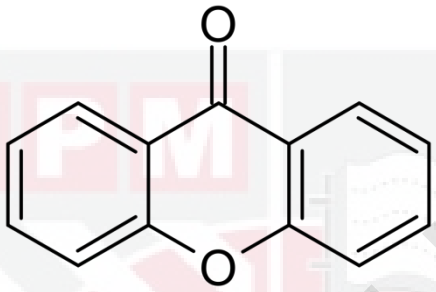

Figure 2.1 : Chemical structure of xanthone (9H-xanthen-9-one)

2.1.1 Bio-Active Functions of Mangosteen

Mangosteen, also known as *Garcinia mangostana*, is a tropical fruit from the Mangosteen family. It is naturally found in countries such as Malaysia, Indonesia, Thailand, Myanmar, Sri Lanka, India, and the Philippines. This fruit is regarded as a superfruit due to its numerous nutritional benefits. A 100-gram serving (including jar and syrup pack) provides approximately 73 calories, 18 grams of carbohydrates, 0.4 grams of protein, 0.6 grams of fat, and 2 grams of fiber (Kalick et al. 2023). The fruit has long been used in traditional herbal medicine due to the phenolic compounds it contains such as xanthones, tannins and pro-anthocyanin (Ridwan et al. 2021). Xanthones play a crucial role in preventing lead-induced chronic kidney disease (CKD) by activating Nrf-2 and modulating the NF-kB and MAPK pathways, thereby improving

tissue architecture. Extracts from the peel of mangosteen have demonstrated a wide range of potent pharmacological properties, including antioxidant, antibacterial, antiviral, antiallergic, antiproliferative, anticancer, and anti-inflammatory effects (Rana et al. 2020).

2.1.2 Components in Mangosteen Pericarp

The pericarp of mangosteen is extensively utilized in medicine owing to its high therapeutic properties. Phytochemical screening has revealed that mangosteen pericarp extract contains saponins, tannins, polyphenols, flavonoids, and xanthones. Among these, xanthones are identified as the primary phenolic compounds present in the mangosteen fruit pericarp. The potent active ingredients within the mangosteen pericarp inhibit the tissue-damaging process and have been used in folk medicine to relieve diarrhea and treat skin wounds and ailments (Vo et al. 2023). Various plant materials, including fruits, vegetables, spices, leaves, roots, and bark, have been extensively studied as potential sources of natural antioxidants.

(Suksamran et al. 2022) assessed the antioxidant activity of several xanthones isolated from mangosteen pericarp. Among these, 8-hydroxycudraxanthone, gartanin, γ-mangostin, α-mangostin, and smeathxanthone exhibited the strongest antioxidant activity.

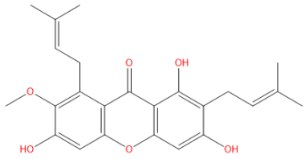

α-Mangostin

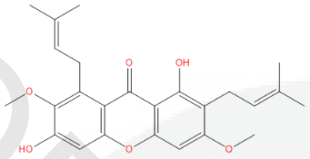

β-Mangostin

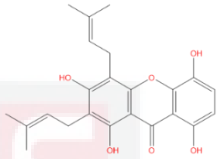

Gartanin

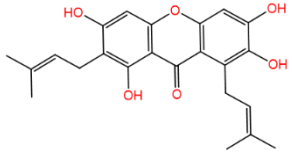

γ-mangostin

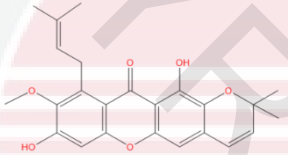

9-hydroxycudraxanthone

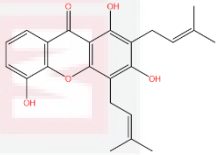

8-deoxygartanin

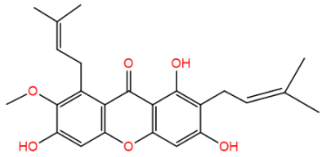

1,3,6-trihydroxy-7-methoxy-2,8-(3-methyl-2-butenyl) xanthone

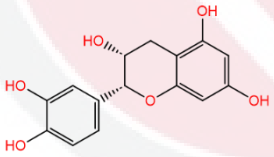

Epicatechin

Figure 2.2 : Some chemical compounds isolated from pericarp and seed of mangosteen (Çalış et al. 2023)

2.2 Virgin Coconut Oil (VCO) as Solvent in Xanthone Extraction

Vegetable oils have been utilized as alternative solvents for eco-friendly extraction, purification, and formulation of food and natural products due to their superior chemical properties. Coconut oil and medium-chain triglycerides (MCTs) derived from coconut oil are particularly favored in the flavor industry because of their higher polarity compared to conventional oils (Prasanna 2024). Unlike other natural oils, coconut oil and MCTs have a lower molecular weight even at low temperatures. They are miscible with hydrocarbons, esters, natural oils, alcohols, ketones, and acids. Additionally, coconut oil is exceptionally stable against oxidation due to its low content of unsaturated fatty acids, which contributes to its excellent preservation qualities and extends the shelf life of finished products. Compared to other oils, coconut oil boasts higher nutritional value and biological activity, with minimal adverse effects on human health. Its richness in medium-chain triglycerides (MCTs) makes it a popular solvent or vehicle for drugs, and it is not associated with heart attacks or other cardiovascular diseases. Coconut oil also boosts the body's metabolism and energy expenditure, as it is directly converted to energy in the liver rather than being stored in fat tissue, indicating its potential in anti-obesity treatments. Additionally, coconut oil is abundant in lauric acid and mono-nucleosides, which can inhibit various pathogenic bacteria such as Listeria monocytogenes, enterotoxigenic E. coli, and Staphylococcus aureus. It also contains phenolic compounds like protocatechuic acid, vanillic acid, syringic acid, p-coumaric acid, caffeic acid, and ferulic acid (Bao et al. 2023).

Virgin coconut oil (VCO) possesses desirable properties for use in final products. For instance, there is no need to separate vegetable oils from the final products obtained after ultrasonic-assisted extraction (UAE), as these oils are safe for consumption and may contain beneficial natural bioactive compounds. With petroleum-derived solvents facing strict global regulations, there is an increasing demand for more environmentally friendly, bio-based, and renewable solvents for the extraction, purification, and formulation of natural and food products. Ideal alternative solvents are non-volatile organic compounds that offer high solvency, high flash points, low toxicity, and minimal environmental impact. These solvents should be sourced from renewable resources at reasonable prices and be easily recyclable. According to the principles of green chemistry and green engineering, vegetable oils can serve as excellent alternative solvents for extracting compounds for purification, enrichment, and even pollution remediation (Yara-Varón et al. 2017).

Research conducted by N. Pujirahayu and colleagues demonstrated that propolis, which contains a diverse range of chemicals such as polyphenols, terpenoids, and amino acids, can be effectively extracted using virgin coconut oil (VCO) and olive oil. The antibacterial activity of these extracts was found to be superior to that of extracts obtained with traditional organic solvents. Utilizing coconut oil as a bio-solvent for extracting bioactive compounds from natural sources represents a strategic approach to amplifying its beneficial properties (Pujirahayu et al. 2015). Furthermore, coconut oil-based extracts can be directly incorporated into various emulsifying foods and cosmetics without the need for solvent removal, offering greater convenience and cost-

effectiveness. Given the significant benefits of this value-added oil, developing coconut oil-based solvents for extracting phenolic bio-oil products will enhance its value. However, our preliminary studies indicate that coconut oil alone has limited efficacy in extracting phenols from MP. To address this, we propose using a mixture of ethanol and virgin coconut oil (VCO) as solvents to improve the extraction rate of xanthones while retaining the advantages of VCO.

2.3 Effect of Mixed-Solvents on Xanthone Extraction

In the experimental results of using virgin coconut oil (VCO) as a single solvent to extract xanthone from mangosteen pericarp, it can be observed that the yield of xanthone was low (Zhang et al. 2021). In previous studies, it was found that the solubility of xanthone in ethyl acetate and ethanol was relatively high, and the reason was explained that these solvents had more suitable hydrogen-bond basicity and di-polarity/ polarizability than VCO. In this study, ethanol was selected as the co-solvent of VCO, because ethanol has a higher hydrogen bond donating ability than ethyl acetate, which will promote the solvent molecule to be more compatible with the carbonyl group on the central ring and the oxygen atoms of biaryl ether groups. Good binding, thus improving the extraction rate (Lee et al. 2019). Ethanol, being a hydrophilic organic solvent, effectively dissolves a wide range of chemical components, making it suitable for comprehensive extraction. For instance, 95% ethanol is ideal for extracting alkaloids, essential oils, resins, and green leaves, while 60% to 70% ethanol is better suited for extracting glycosides. Even at lower concentrations, ethanol can efficiently extract polysaccharides, proteins, and other compounds (Du et al. 2023). The extract has low viscosity, easy filtration

and easy concentration. Ethanol has relatively low toxicity among common organic solvents and was easy to separate from the extract at the end of the extraction process. Ethanol was easily available and cheap, giving it a price advantage in large-scale industrial production (Vargas-Campos et al. 2023).

2.4 Advantages of Mixed-Solvents

Mixed-solvents are usually used to increase the selectivity and distribution coefficient of the target compound in the solvent. In addition, the method of pairing hydrogen bond donors and acceptors was often used in the selection of solvent species. However, the existence of hydrogen bonds was not a sufficient factor to improve the extraction rate, and the difference in interrelationship between solute and solvent caused by inter-molecular forces and polarity differences needs to be considered. From this perspective, binary or ternary mixed-solvents with suitable components can have a higher interrelationship than a single solvent, which provides the possibility to improve the extraction rate and selectivity of the target compound in the solvent (Zhao et al. 2023). In a multisolvent system, there are distinct interactions such as hydrogen bonds and non-specific interactions like dipole-induced and dipole-dipole interactions between each solvent. These interactions establish a unique polar environment within the mixed-solvent system, influencing the synergies among the solvents. This, in turn, enhances the solubility of the solute (Lee et al. 2023).

Based on the principle of "like dissolves like", a single solvent system was the first choice for chemical synthesis. However, some dissolution occurring in

mixed-solvents systems has been observed to have better solubilitycharacteristics than single solvent. So far, mixed-solvents systems have been widely used for many years, especially in the field of extraction. For example, by choosing a solvent through a computer program, it was now easy to predict how a given organic compound will dissolve in a mixture of two solvents. While mixed solvents are commonly employed in the extraction of organic compounds, there is limited research on the principles for selecting these mixed solvents. Solvents are crucial to the success of chemical reactions, and since many natural reactions occur in mixed-solvent systems, a methodical approach to choosing mixed solvents is essential. The impact of mixed solvents on chemical synthesis can be assessed by calculating the Hansen solubility parameter (HSP) distance R_a, which is derived from dispersive, polar, and hydrogen-bonding solubility parameters (Mihalovits 2022). For instance, in the synthesis of polydopamine (PDA) within a water-alcohol system, well-dispersed PDA spheres were achieved using solvents with smaller R_a values. Additionally, mixed solvents with smaller R_a values resulted in higher dopamine conversion. Thus, employing a mixed-solvent selection strategy based on R_a values can assist in choosing the optimal reaction medium for more efficient chemical synthesis.

2.5 Ultrasound-Assisted Extraction (UAE)

One of the important steps in the study of medicinal plants was extraction. Currently, several modifications are being made to conventional methods of processing pharmaceutical products with the aim of increasing yields at lower cost. Ultrasound-assisted extraction (UAE) is one of such modification (De

Laet et al. 2024). There are many extraction methods to extract xanthone. Ultrasound-assisted extraction (UAE) has gained significant attention for its benefits, including low energy consumption, short extraction times, high efficiency, gentle heating temperatures, and minimal damage to active ingredients during the process. The fundamental principle behind UAE involves utilizing the resonance and cavitation effects produced by ultrasound waves to disrupt plant cell walls, facilitating the penetration of the solvent into the cells. This enhances the dissolution of xanthones and improves the overall extraction efficiency. Initially, ultrasound waves rapidly disrupt the fibrous surface of the mangosteen pericarp. Subsequently, the vibrations enhance the uniform release of xanthones from the pericarp, dispersing them into the solvent for more effective dissolution and extraction. This approach, when combined with solvent extraction, offers a promising method for the rapid extraction of high-yield phenolics. Additionally, the ultrasound extraction process helps mitigate the impact of high temperatures on the active substances during extraction (Agarwal et al. 2018). The remarkable advantages of ultrasound-assisted extraction (UAE) have fueled its advancement in extracting biological compounds like lipids. Traditional lipid extraction is often hindered by intact and rigid cell walls and the formation of complexes between nonpolar molecules and polar lipids, which slow down extraction kinetics. UAE effectively promotes the release of cellular lipids and accelerates the extraction process. It has proven to be a viable alternative to conventional extraction methods, significantly enhancing the yield of xanthones compared to traditional techniques. Additionally, UAE reduces extraction times, leading to improved overall extraction efficiency (Tang et al.

2023). Khursheed et al. optimized the extraction process of active ingredients from Centella asiatica using ultrasound-assisted extraction (Khursheed et al. 2024).

Consumers are increasingly focused on the health food industry, making research on ultrasound-assisted extraction of organic compounds, such as xanthones from mangosteen pericarp, highly significant for advancing related fields. This project aims to delve into various aspects of ultrasound-assisted extraction (UAE), including its mechanisms, solvent systems optimized for ultrasound, the use of mixed solvents, and the effects of cavitation rate and pulse time on extraction rates. The focus is on understanding how UAE enhances extraction efficiency and its implications for further development in this field.

Currently employed techniques for xanthone extraction encompass a range of methods, including hot water extraction, microwave-assisted extraction, deep eutectic solvent extraction, subcritical ethanol extraction, liquefied dimethyl ether extraction, and supercritical carbon dioxide ($scCO_2$) extraction with the aid of organic co-solvents, among others. Different extraction techniques have certain specific disadvantages. For example, the process of supercritical carbon dioxide extraction was complicated, the extraction time was long, and the extraction rate was low. Microwave-assisted extraction was difficult to precisely control the conditions of the extraction process, and it was impossible to conduct precise control variable research, and the temperature

of the microwave extraction system was high, which was easy to cause damage to the structure and properties of the experimental materials.

As an important and valuable bioactive compound, xanthone has garnered significant attention from researchers. In recent years, a range of xanthone extraction technologies has been utilized for separating xanthones and α-mangostin from biomass components. These methods include microwave-assisted extraction, supercritical carbon dioxide ($scCO_2$) extraction, and ultrasound-assisted extraction (UAE). Table 2.1 presents the xanthone extraction rates achieved with different extraction techniques in previous studies. These techniques have effectively isolated xanthone from mangosteen pericarp, with microwave-assisted extraction using 71% ethanol yielding 100.48 ± 2.12 mg/g of α-mangostin (Mohammad et al. 2019). It is noteworthy that ethanol is commonly used across various separation techniques and has proven effective in increasing the yield of xanthone.

Table 2.1 : Summary of different processes and conditions of xanthone extraction

Technique	Sample	Solvent	Co-solvent	Solute & solvent ratio	Target compound	Operation conditions	Extraction yield	References
$scCO_2$	Mangosteen pericarp	$scCO_2$	40% Virgin coconut oil	-	xanthone	T: 70°C t: 420 min P: 430 bar	xanthone in MPE: 32.6 mg/g	(Siew et al., 2021)
Microwave-assisted extraction (MAE)	Mangosteen pericarp	71% Ethanol	-	25 mL/g	xanthone	t: 2.5 min	α-mangostin: 100.48 ± 2.12 mg/g	(Nor Azizah et al., 2019)
Microwave-assisted extraction (MAE)	Garcinia mangostana	Ethanol	-	1:8	α-mangostin	Ethanol concentration: 95% T: 70°C T: 10 min	α-mangostin: 9.9%	(Lei Fang et al., 2011)

T: temperature; t: time; P: pressure

Table 2.1 : Continued

Technique	Sample	Solvent	Co-solvent	Solute & solvent ratio	Target compound	Operation conditions	Extraction yield	References
Water bath heating extraction	Cyclopia genistoides	Water	Ethanol	10 mL/g	xanthone	T: 70°C Water: ethanol ratio: 1:1 (v/v)	Xanthone yield: 4.02 ± 0.03 g/100 g	(Stephanie C. Bosman et al., 2017)
Subcritical water extraction	Mangosteen pericarp	Subcritical water	30% deep eutectic solvent	-	xanthone	T: 160°C P: 10 MPa	Xanthone yield: 27.15 mg/g	(Siti Machmudah et al., 2018)
$scCO_2$	Mangosteen pericarp	$scCO_2$	20% Virgin coconut oil	-	α-mangostin	T: 60°C P: 35 MPa	α-mangostin: 9.25 ± 0.21%	(Lee et al., 2019)
Heated reflux	Garcinia mangostana	Ethyl acetate	-	10 mL/g	α-mangostin	T: 77°C t: 1 h	α-mangostin: 4.19 g/100 g	(Kunnitee et al., 2015)

T: temperature; t: time; P: pressure

Table 2.1 : Continued

Technique	Sample	Solvent	Co-solvent	Solute & solvent ratio	Target compound	Operation conditions	Extraction yield	References
Aqueous micellar biphasic system (AMBS)	Garcinia mangostana pericarps	Water	Pluronic L-81	-	mangostin	T: 40°C pH: 8 3% (w/w) Pluronic L-81	α-mangostin: 2646.6 ± 1.2 µg/mL	(Grace Yin Tze Tan et al., 2016)
Ultrasound assisted extraction (UAE)	Mangosteen pericarp	Ethanol	-	20 mL/g	xanthone	T: 33°C t: 1 h Amplitude: 50% 50% ethanol	Xanthone: 0.16 mg/g	(Nuttawan et al., 2012)

T: temperature; t: time; P: pressure

Table 2.2 presents a summary of the characteristics of various commonly utilized assisted processes for extracting xanthone from mangosteen pericarp, including extraction efficiency, environmental impact and material cost

Table 2.2 : Comparison of several previous methods for extracting xanthone

Method	Advantage	Shortcomings
$scCO_2$ extraction	● Avoid traditional organic solvents that pose higher toxicity risks to products. ● By adjusting the temperature or pressure, the extract can be quickly separated.	● It is not suitable for substances with high polarity and high molecular weight. ● The extraction rate of target components is generally not high.
Microwave-assisted extraction (MAE)	● Microwave has strong permeability and selectivity. ● Extraction times are shorter and require less solvent volume. ● High environmental friendliness.	● Extraction parameters are not easy to set precisely. ● Microwaves have the potential to affect the properties of materials.
Heated reflux	● The extraction equipment is simple. ● The extraction process is gentle and does not alter the properties of the material.	● The extraction time usually takes more than 1 h. ● The extraction rate is relatively low.
Ultrasound assisted extraction (UAE)	● The extraction time is short. ● The extraction rate is higher due to the penetration and fragmentation of the plant material by ultrasound. ● The extraction parameters of UAE can be precisely controlled to facilitate quantitative studies.	● Because of the heating effect of ultrasound waves, UAE has higher requirements on the amount of solvent. ● Noise during extraction.

2.6 Ultrasound Assisted Extraction Model

Peleg Model

In 1988, Peleg introduced a two-parameter sorption equation, known as the Peleg model, and evaluated its predictive accuracy in the context of water vapor adsorption for milk powder and whole rice, as well as the soaking of whole rice. Since then, the Peleg model has been widely employed to describe sorption processes across various food products. Peleg model is a popular empirical non-exponential model whose parameters have important practical significance in applying hydration dynamics to weight gain during rehydration. (Shafaei et al. 2016) utilized the Peleg model to analyze water absorption during the soaking of beans and chickpeas. Similarly, (Izza et al. 2023) applied the model to evaluate the efficiency of microwave-assisted extraction of proanthocyanidins from red sorghum grains, investigating the effects of varying microwave power and citric acid concentrations.

Pseudo-Second-Order Kinetic Model

In order to study the dissolution mechanism for better extraction efficiency, previous researchers proposed several dissolution kinetic models to express the dissolution mechanism of solutes in solvents. Among these dissolution kinetic models, the pseudo-second-order kinetic model is the most popular model and has been widely used in many dissolute kinetic studies. This model has been applied to various adsorption systems, from biomass to nanomaterials as adsorbents and from heavy metals to pharmaceuticals as adsorbates or pollutants. Over the past few decades, equational expressions for pseudo-second-order models have been derived to simplify calculations.

In these equational expressions, the derived equations of the form are often used to investigate the correlation of dissolution data with pseudo-second-order kinetic models due to their simplicity and good fit to many dissolution studies over the past decade (Moussout et al. 2018, Regazzoni 2020, Cortés et al. 2023)

The formula of the above kinetic model and the specific calculation process are presented in detail in Chapter 3.

2.7 Summary

Virgin coconut oil (VCO) has limitations when it comes to extracting xanthones from mangosteen pericarp. However, incorporating ethanol as a co-extractant can enhance xanthone extraction efficiency and improve the interaction between the solute and mixed solvents. Compared to other extraction techniques, ultrasound-assisted extraction (UAE) offers advantages such as reduced extraction time and higher extraction rates. Nevertheless, factors like cavitation rate, extraction duration, and solvent type can influence the results. Various solubility models, along with response surface methodology (RSM) models, are available to predict the kinetics of UAE.

CHAPTER 3

MATERIALS AND METHODS

3.1 Experimental Materials

Virgin coconut oil (VCO) from the Supercoco series (Philippines) was used in this study. Laboratory-grade xanthone (CAS: 90-47-1), with a purity of 97%, was obtained from Sigma Aldrich Company. Mangosteen pericarp was sourced from local orchards in Malaysia. Absolute ethanol (99.90% mass concentration) was procured from John Kollin Corporation. All reagents were of High-Performance Liquid Chromatography (HPLC) grade, including methanol (CAS No. 67-56-1) from Friendemann Schmidt (Malaysia), acetonitrile from JT Baker-Fisher (United States), and ortho-phosphoric acid (CAS No. 7664-38-2) from Systerm (Malaysia).

3.2 Sample Storage and Handling

Mangosteen pericarp was dried at 60°C until 15% moisture content. The dried pericarp was ground into powder sieved to obtain uniform particle sizes. For this study, particles sized at (250 - 425) μm were selected. All samples were securely stored in a cold room, sealed, and protected from light.

3.3 Solubility Determination of Xanthone

Solubility testing serves to provide a more precise understanding of the solubility of xanthone in various solvents and mixed-solvents with differing solvent ratios. The outcomes of solubility testing offer valuable insights for

selecting optimal mixed-solvents ratios and determining the appropriate balance between materials and solvents. Additionally, solubility testing establishes a factual foundation for assessing the suitability of combining two solvents.

The solubility experiment was performed based on a reference from (Abdkarimi et al. 2021). 3 g of xanthone was added to a vial containing 20 mL of a virgin coconut oil (VCO) and ethanol mixture, with volume ratios ranging from 0 to 1. The vial was properly sealed and maintained at the desired temperature range (303.15 - 323.15) K using a water bath. The sample was continuously stirred for 6 h with a magnetic stirrer. To ensure that ethanol evaporation did not occur during the experiment, an additional sealed vial containing ethanol was monitored, and any mass changes of the ethanol were recorded as a precautionary measure. After reaching equilibrium at the set temperature, a portion of the sample was withdrawn and filtered to remove the excess xanthone, and the absorbance was recorded at 347 nm using a UV-vis spectrophotometer (Genesys 10S, Thermo Scientific, U.S.A). The xanthone concentration was calculated based on calibration curves (Figure S1). The solubility measurement was performed in duplicate.

A mixed-solvents of Virgin Coconut Oil (VCO) and Ethanol was prepared by combining precise volumes of VCO and ethanol in a proportion that yielded a total volume of 20 mL of solvent. The solubility of xanthone was ascertained by titrating excess xanthone standard with binary solvent mixtures. For this purpose, 3 g of xanthone was introduced into the mixture and maintained at a

desired temperature range (303.15 - 323.15) K using a water bath. Simultaneously, the sample underwent continuous stirring and dissolution for 6 h under the influence of a magnetic stirrer. To account for the volatility of ethanol, a 50 mL capacity beaker was employed during the dissolution process, with its top securely sealed using film and tin foil to ensure constant solvent proportions. Upon reaching equilibrium at a defined temperature, a portion of the sample was filtered to obtain a saturated solution for subsequent solubility tests. The same dissolution methodology was applied to the control group, with a dissolution time of 48 h, confirming the attainment of equilibrium. This process was iterated for all measured temperatures. Gradient difference solutions were prepared by introducing specific quantities of xanthone into mixed-solvents with varying proportions. Calibration curves were generated for mixed-solvents of different ratios, and the experiment was replicated three times for each concentration. The filtered saturated solution was diluted according to the original mixed-solvents ratio. The UV-vis spectrophotometer recorded the absorbance at 347 nm, and the concentration of xanthone was computed based on the calibration curve established by the absorbance of the standard solution.

The Jouyban-Acree model was used to describe the relationship between the mass fraction solubility of xanthone and both temperature and the initial binary solvent composition of mixtures containing virgin coconut oil (VCO) and ethanol. The equation for this model is given by:

$$lnx_3 = w_1 lnx_1 + w_2 lnx_2 + \frac{w_1 w_2}{T} \sum_{i=0}^{2} J_i (w_1 - w_2)^i \quad (3.1)$$

In the equation, x_3 represents the experimental solubility of xanthone in the solvent, while x_1 and x_2 denote the solubility of xanthone in pure virgin coconut oil (VCO) and pure ethanol, respectively, at the absolute temperature T. The parameters w_1 and w_2 indicate the solute-free volume fractions of VCO and ethanol in the initial binary mixtures without the solute. The parameters J_i (where i corresponds to J_0, J_1, and J_2 are model-specific constants.

In this study, mixture of VCO-ethanol was used as a solvent system. VCO being a combination of various fatty acids, adds complexity to the system compared to simple binary solvents. Therefore, Jouyban-Acree model was modified to have better consideration for these complexities. These modifications included considering the absolute value of solubility differences and using w_{1max} (the solute free volume fraction of VCO at the highest observed solubility) instead of w_2 in the model.

Virgin Coconut Oil (VCO), being a composite of diverse fatty acids, introduces heightened interactions and system complexity compared to typical binary solvents when combined with ethanol to formulate a solvent system. The Jouyban-Acree model has undergone partial modifications to emulate the internal variations within solvents possessing different volume fractions. These adjustments involve incorporating the absolute value of the solubility difference and substituting w_2 with w_{1max} (the w_1 value at the highest solubility, as observed from experimental data). The solute free volume fraction of VCO corresponding to the highest solubility point of xanthone signified the

proportion of VCO in the solvent system that contributed most significantly to the interaction within the solution system.

$$lnx_3 = w_1 lnx_1 + w_2 lnx_2 + \frac{w_1 w_2}{T}\sum_{i=0}^{2} J_i |w_1 - w_{1max}|^i \quad (3.2)$$

Eq. (3.2) was evaluated with data from previous experiments in different binary solvent systems. The results show that Eq. (3.2) has excellent ability to fit the solubility of each target compound in the binary solvent system (Figure S2-4).

To assess the accuracy of the prediction model, the Relative Mean Deviation (Gupta et al. 2016) was computed at four distinct temperatures (303.15 K, 308.15 K, 313.15 K, and 323.15 K). The correlation was performed with solver in Microsoft Excel and relative mean deviation (RAD) was used as an objective function (Eq. 3.3):

$$RAD = \frac{1}{N}\sum_{i=1}^{N}\left(\frac{|x_c - x_3|}{x_3}\right) \quad (3.3)$$

Where x_3 is the experimental mass fraction solubility value and x_c is the mass fraction solubility value calculated by the prediction model. N is the number of experimental data.

To assess whether the effect of temperature on the solubility of xanthone is linear, the relative standard deviations (RSD) of 11 groups of solvents with different compositions were calculated using the following formula:

$$RSD = \frac{\sqrt{\frac{1}{N}\sum_{i=1}^{n}(x_i - W)^2} \times 100}{W} \quad (3.4)$$

Where N is the number of solvents were used in each temperature. x_i is the mass fraction solubility of xanthone on different temperature. W stands for the mean value of solubility data of each group.

3.4 Viscosity and Density Measurement of Mixed-Solvents, and Data Correlation

A HAAKE Viscotester E Rotational Viscometers was used to measure the viscosity of different solvents and the effect of solvent mixture on viscosity. The viscosity of three distinct solvents utilized in Ultrasound-Assisted Extraction (UAE) at 302.55 K was determined using a rheometer. All of the viscosity measurements were conducted at a shear rate of 1551.9 s^{-1}.

The density of pure virgin coconut oil (VCO), ethanol, and their binary mixture with different VCO volume fractions was measured using a digital density meter (Anton Paar DMA 1001) with a repeatability of 1×10^{-5} g/cm^3 and 0.01 K, maintaining atmospheric pressure for all systems investigated in this study. 5 mL of sample was injected and ensuring the absence of air bubbles. The measurements were conducted at 323.15 K to prevent the solidification of VCO, which could potentially alter the ratio and properties of VCO and ethanol mixtures.

The Redlich-Kister model is shown in Eq. (3.5) to represent the behavior of density of Virgin coconut oil and ethanol mixture with composition.

$$\rho_{mix} = \rho_{id} + \rho_{ex} \tag{3.5}$$

In this context, ρ_{mix} represents the density of the mixture, ρ_{id} denotes the density assuming ideal behavior, and ρ_{ex} includes the excess term, which accounts for deviations from ideal behavior.

Using the additive behavior approach, the ideal behavior of density is given in Eq. (3.6) as:

$$\rho_{id} = \frac{\sum x_i MW_i}{\sum \frac{x_i MW_i}{\rho_i}} \tag{3.6}$$

where MW_i refers to the molecular weight of component i and x_i represents the mole fraction of component i. This expression essentially represents the ratio of the average molar mass to the average molar volume.

Equation (3.7) illustrates the excess term using the Redlich-Kister expansion, a model that accommodates the non-ideal density behavior in systems comprising two components, denoted as A and B.

$$\rho_{ex} = x_A x_B \sum_{j=1}^{n} (A_j + B_j T)(x_A - x_B)^{j-1} \tag{3.7}$$

where j defines the order of the expansion. A_j and B_j define the j-th order binary interaction parameter between A and B.

Excess molar volumes (V^E) have been evaluated using Eq (3.8):

$$V^E = \frac{\sum_{i=1}^{n} x_i M_i}{\rho} - \sum_{i=1}^{n} \frac{x_i M_i}{\rho_i} \tag{3.8}$$

Where x_i denotes the mole fraction of the pure component, M_i is the molar mass of the pure component, ρ represents the density of the mixture, ρ_i is the density of the respective pure component n is the number of components present in the system.

3.5 Control Group Extraction of Mangosteen Pericarp

To assess the impact of solvent type, mixed-solvents ratio, and ultrasound assistance on the extraction of xanthone form mangosteen pericarp, three control extraction groups were conducted in this study. In the first control group, 3 g of mangosteen pericarp powder was introduced into a mixed-solvents of virgin coconut oil (VCO) and ethanol in a volume ratio of 6:4. The sample from this control group underwent continuous stirring on a magnetic stirrer at 60°C and 300 rpm for 3 h. The resulting supernatant, obtained after centrifugation, was sealed for subsequent detection. The objective of this control group was to investigate the extraction efficiency of xanthone in mangosteen pericarp using mixed-solvents without ultrasound assistance. The other two control groups underwent ultrasound-assisted extraction with VCO and ethanol, each maintaining the same parameters. Following the completion of extraction, the samples were stored similarly for further concentration measurement.

3.6 Ultrasound-Assisted Extraction (UAE) with Mixed-Solvents of Ethanol and Virgin Coconut Oil (VCO)

The ultrasound generator amplifies the extraction efficiency of target components in the material through the cavitation effect induced by the implosion of bubbles generated during the intense vibration of the sample

liquid. The yield of Ultrasound-Assisted Extraction (UAE) often surpasses that of soxhlet extraction due to this cavitation effect. In contrast to the supercritical carbon dioxide extraction method, the UAE process proves simpler and swifter. Furthermore, in comparison with microwave-assisted extraction, which also boasts high efficiency, the parameters of UAE are more easily and precisely controlled, minimizing the likelihood of unpredictable alterations in the physical and chemical properties of materials. The Sonicator operates at a frequency of 20 kHz and has a maximum power output of 500 W, fitted with 18 mm diameter horn was used to generate the ultrasound effect and extract bioactive substances from plant material. A centrifuge (Kubota 2420, Tokyo, Japan) was used to process the supernatant after ultrasound extraction to obtain a pure saturated solution.

The ultrasound-assisted extraction (UAE) experiment was conducted using a VCO:ethanol mixed-solvents (6:4 volume ratio) as well as pure ethanol and VCO, with a mangosteen pericarp powder to solvent ratio of 3:100 (g/mL). The extraction took place in a jacketed beaker (diameter=50 mm, height=100 mm). Ultrasound was applied using a sonicator (Q500 Probe sonicator, Qsonica, U.S.A) with a pulse on-time of 7 s and a pulse off-time of 2 s. The horn was submerged 10 mm below the surface of the solvent. Five extraction durations were tested: (5, 10, 15, 20, and 25) min. Ultrasound power levels of 17 W, 21 W, and 26 W were used. The energy efficiency of the ultrasound was calibrated and is shown in the appendix. The temperature of the extraction system was recorded until the extraction was completed. To prevent ethanol evaporation during the UAE process, the extraction container was sealed with

film and an insulator. After the extraction was complete, the solution was transferred to a 50 mL centrifuge tube. The samples were centrifuged at 4000 rpm for 15 min, and after centrifugation, the supernatant was collected and stored at 4°C until concentration testing.

The cavitation of the solution by the ultrasound wave generates significant heat, expediting the release of active ingredients in the mangosteen pericarp into the solvent. To account for this, the initial temperature of the UAE was set to room temperature (300.55 K), and the extraction process recorded the actual final temperature upon completion. To prevent the evaporation of ethanol during the UAE process, the extraction container was sealed with film and cardboard.

Considering the evaporation temperature of ethanol, the ultrasound intensity was set to 17 W, 21 W, and 26 W (the output power of the ultrasound generator when the amplitude percentages were 20%, 25%, and 30%, respectively) to ensure that the proportion of the mixed-solvents did not change significantly at the final temperature.

3.7 Total Xanthone Content Measurement

The concentration of xanthones in mangosteen pericarp extract (MPE) was assessed using a UV-vis spectrophotometer (genesys 10S UV-vis spectrophotometer, Thermo Scientific, U.S.A) at wavelength of 324 nm. 0.5 cm thick quartz cuvette was used to fill the sample.The calibration curve was

established with the xanthone standard substance in the solvent employed in this experiment (Figure S1).

$$xanthone\ concentration\ in\ MPE, mg/g = \frac{mass\ of\ xanthone}{mass\ of\ MPE} \quad (3.9)$$

$$xanthone\ recovery, \% = \frac{xanthone\ extracted\ from\ UAE}{xanthone\ extracted\ from\ soxhlet} \times 100\% \quad (3.10)$$

3.8 Ultrasound- Assisted Extraction (UAE) Kinetic Study

In this study, two mathematical models, the Peleg model and the Pseudo-Second-Order Kinetic model, were employed to study the extraction kinetics of xanthone from mangosteen pericarp.

Peleg's Model

A significant advantage of Peleg's model is its ability to utilize short-term experimental data to predict the equilibrium concentration of a dissolved system (Milićević et al. 2021). The Peleg's model is expressed as follows:

$$C_t = C_0 + \frac{t}{(k_1 + k_2 \times t)} \quad (3.11)$$

where C_t is the sample concentration (mg/mL) at time t, C_o is the initial sample concentration (mg/mL), t is time (min), k_1 (min mL/mg) and k_2 (mL/mg) are the Peleg rate and Peleg capacity constant respectively. It can be seen that k_1 is the inverse of the initial concentration, and k_2 determines the final sample concentration.

Pseudo-Second-Order Kinetic Model

The pseudo-second-order equation is generally written as below (Huang et al. 2018):

$$\frac{dC_t}{dt} = K(C_e - C_t)^2 \quad (3.12)$$

where C_t (mg/g) is the concentration at time t (min), C_e is the concentration at equilibrium (mg/mL) and K, is the rate constant of the pseudo-second-order dissolution (min^{-1}). The driving force of the process is $(C_e\text{-}C_t)^2$.

Eq (3.13) can be rearranged to obtain a linearity form as follows:

$$\frac{1}{(C_e - C_t)} = \frac{1}{C_e} + Kt \quad (3.13)$$

Eq (3.13) is the first linearized type of pseudo-second-order equation. It has $1/(C_e\text{-}C_t)$ on the Y axis and t on the X axis for the linearized Eq (3.13). Eq (3.13) can be converted to another alternative linearity form as follows:

$$C_t = C_e - \frac{1}{KC_e}\frac{C_t}{t} \quad (3.14)$$

It has C_t on the Y axis and C_t/t on the X axis for the linearized Eq (3.14).

An R^2 value close to unity indicates a strong correlation between the experimental results and the predicted data, reflecting a better fit. The Peleg model, along with pseudo-first-order type 1 and type 2 models, was solved using the SOLVER tool in Microsoft Excel 2010. An R^2 value near 1 was used as the criterion to assess the agreement between the experimental data and the models. This criterion is calculated as follows:

$$R^2 = \left[\frac{\sum_{n=1}^{N}\left(C_{L,exp,n} - C_{L,pre,n}\right)^2}{\sum_{n=1}^{N}\left(C_{L,exp,n} - \overline{C_{L,exp}}\right)^2}\right] \quad (3.15)$$

3.9 Morphology Analysis of Mangosteen Pericarp Residues from Ultrasound-Assisted Extraction (UAE)

In order to study the effect of solvent type used in ultrasound assisted extraction (UAE) on the morphology of mangosteen peel, 4 groups of samples were selected for SEM analysis. These included a control group without UAE treatment, group 1 with virgin coconut oil (VCO) as the solvent, group 2 with ethanol as the solvent, and group 3 with a mixture of VCO and ethanol (6:4 by volume ratio). UAE parameters of groups 1, 2 and 3 were as follows: extraction time 25 min, amplitude percentage 30%, mass of mangosteen peel particles 3 g, solvent volume 100 mL. After extraction, the mangosteen pericarp powder was fully precipitated, the extraction residue at the bottom was collected, and the residual VCO was eluted with ethanol, and then dried in the oven, the ethanol was removed, and the dried mangosteen peel granules were obtained. At least 3 different shapes of mangosteen peel particles were selected for observation in each group. The sample is placed in the holder and inserted into the microscope. The morphology of the sample was observed at 500x and 1000x magnification.

CHAPTER 4

RESULTS AND DISCUSSION

4.1 Solubility of Xanthone in Binary Solvents

Table 4.1 shows the solubility of the xanthone in mixture of virgin coconut oil (VCO) and ethanol across four temperatures (303.15 K, 308.15 K, 313.15 K, and 323.15 K). The corresponding solubility profiles are illustrated in Figure 4.1. The maximum solubility occurred at ratio of 6:4 (VCO: ethanol), while the lowest solubilities were observed at pure VCO and ethanol, both showing approximately the same value. This synergistic effect of mixed-solvent in solubilizing bio-active compounds is commonly reported by other studies (Lee et al. 2023), (Jeong et al. 2022), (Ha et al. 2019), (Wani et al. 2017). These trends were consistent across temperatures from 303 K to 323 K. The observed synergistic effect of the mixed-solvent may be attributed to solvent-solvent interactions, as studied by (Polok et al. 2022), in the case of methanol and chloroform. However, in this study, VCO represents a complex mixture of fatty acids, making the investigation of solvent-solvent interactions complicated. At a given solvent's ratios, solubility of xanthone was increased as temperature increase from 303 K to 323 K. This trend was also commonly reported by others (Preston et al. 2024).

As reported by Kusmayadi et al., ethanol shows superior efficacy as a solvent for extracting xanthones from mangosteen pericarp compared to other studied solvents, which encompass both polar and non-polar types (Kusmayadi 2018). The mixture of VCO-ethanol (6:4), identified in this study, could be exhibit even

greater potential as a solvent for xanthone extraction from mangosteen pericarp.

The relative standard deviations (RSDs) of 11 groups of different constituent solvents were calculated. It is evident that all the results are below 5, indicating the accuracy of the measured solubility data.

Table 4.1 : Mass fraction solubility (x_m^{exp}) values measured for xanthone in virgin coconut oil (VCO) + ethanol solvent mixtures at different temperatures

x_1	Mass fraction × 10^3			
	303.15 K	308.15 K	313.15 K	323.15 K
0.000	11.251	11.831	12.390	13.549
0.113	12.002	12.747	13.497	14.581
0.222	12.928	13.734	14.546	15.902
0.329	14.397	15.273	16.155	17.896
0.433	16.679	17.897	19.122	21.547
0.534	20.004	21.537	23.135	26.244
0.632	24.991	27.043	29.104	33.252
0.728	18.537	19.702	21.395	23.814
0.821	14.971	15.669	16.417	17.884
0.912	12.764	13.336	13.869	14.990
1.000	11.602	12.045	12.492	13.395

Note: x_1 is the solute free volume fraction of VCO in mixed-solvent; all of solubility values are average value; The standard deviation (SD) of all solubility data is shown in table S3; n=2.

Figure 4.1 illustrates the correlation results for the original and modified Jouyban-Acree models regarding the solubility of xanthone in a VCO and ethanol mixture. The results indicate that the modified Jouyban-Acree model provided a better fit for the solubility data of xanthone, while the original Jouyban-Acree model was less effective in predicting the solubility accurately. This discrepancy is likely due to the fact that VCO is a complex mixture of various fatty acids, making the original Jouyban-Acree model—typically used for binary pure solvent systems—less suitable for predicting solubility in intricate mixed-solvent systems. The fitting parameters for the modified Jouyban-Acree model are detailed in Table 4.2. Across all tested temperatures, the Relative Mean Deviation between model predictions and experimental data remains consistently below 0.015, with R^2 values surpassing 0.995.

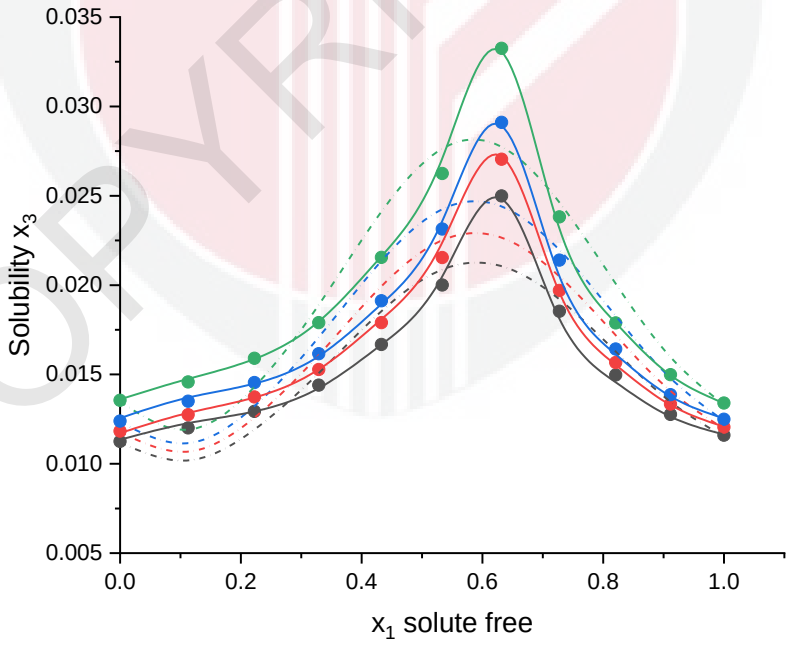

Figure 4.1 : Solubility of xanthone (x_3) in mixture of virgin coconut oil (VCO) (x_1) and ethanol (x_2). Marker: experimental data; Solid line: modified Jouyban-Acree model; Breaking line: Jouyban-Acree model; — (303.15 K); — (308.15 K); — (313.15 K); — (323.15 K)

Table 4.2 : Regression results and model fitting parameter values of the modified Jouyban-Acree model for correlating the solubility of xanthone in a mixture of virgin coconut oil and ethanol (ratio ranging from 0 to 1)

T, K	303.15	308.15	313.15	323.15
J_0	1008.029	1072.935	1141.673	1250.319
J_1	-3422.213	-3486.286	-3733.261	-4009.852
J_2	3703.396	3506.015	3922.352	4075.691
RAD	0.009	0.007	0.006	0.006
R^2	0.998	0.998	0.998	0.998

4.2 Viscosity, Density and Excess Molar Volumes of Virgin Coconut Oil (VCO) and Ethanol Mixture Study

As shown in Figure 4.2, the viscosity of the solvent gradually increased with the rise of the VCO volume ratio, measuring 0.94 mPas, 9.9 mPas, and 36.5 mPas for ethanol, VCO-ethanol (6:4), and VCO, respectively. Viscosity data were correlated by Redlich-Kister model. The fitting parameters are shown in the appendix. A clear observation is that as the ratio of VCO increased, the rate of increase in solution viscosity gradually intensifies.

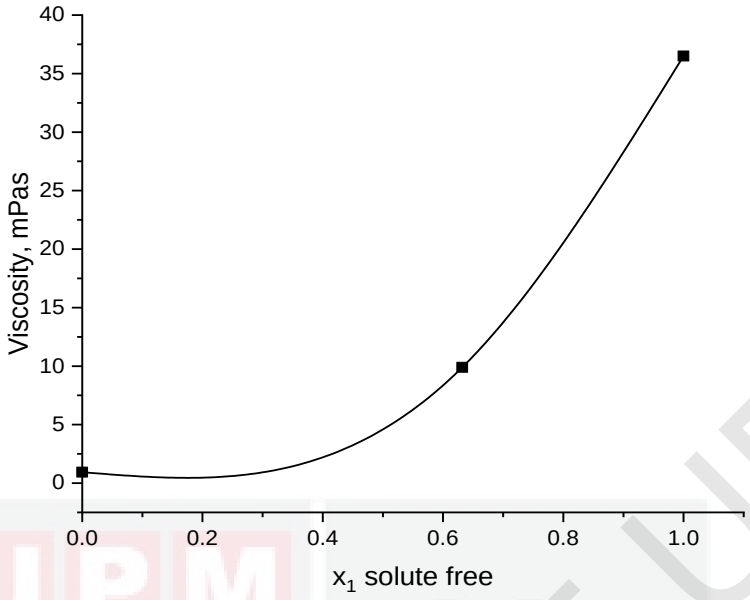

Figure 4.2 : Viscosity of virgin coconut oil (VCO), pure ethanol, and mixture at 302.55 K and shear rate=1550.9 s^{-1}, x_1 represents the solute free volume fraction of the VCO in the mixed-solvent. Marker: experimental data; solid line: Redlich- Kister model

Fig. 4.3 illustrates the densities of the VCO-ethanol mixture at 323 K. The densities of the mixed-solvents exhibited a linear increase with the overall rose in the proportion of VCO. However, within the fraction range of 0.4 to 0.8 of VCO, the density displayed a convex trend, reaching its maximum at x_1=0.6. This deviation from linearity suggests possible molecular rearrangement or structural repacking when VCO and ethanol are mixed. At lower fractions, the dominance of one component may induce a more order arrangement, resulting in a linear relation between density and fraction. In the mid-range fraction (0.4-0.8), a balance in interaction energies between VCO and ethanol could lead to the observed convex density trend. Alam et al. also observing the convex trend densities in the mixed-solvent (Alam et al. 2018). The Redlich-Kister model fitting parameters of density data were obtained synchronously by the calculation of excess molar volume (V^E).

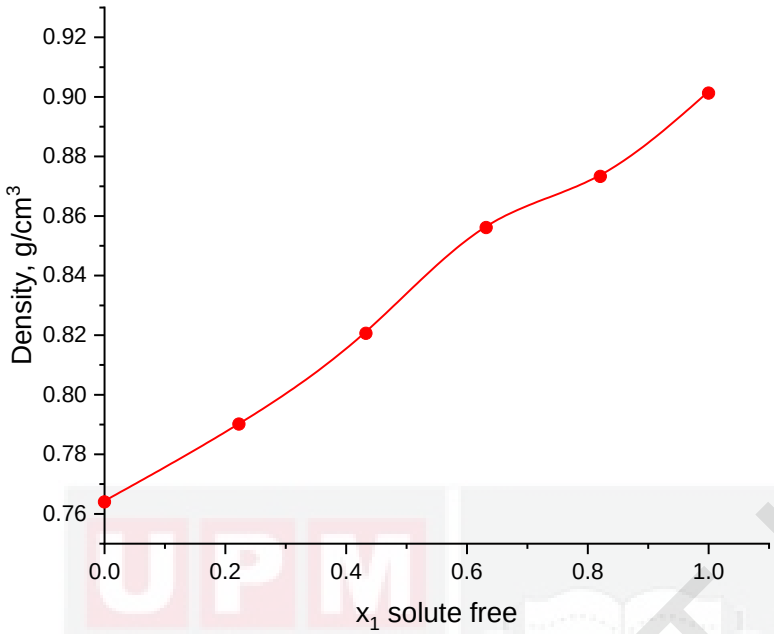

Figure 4.3 : Density of binary mixed-solvent of virgin coconut oil (1) +ethanol (2) at 323.15 K. Marker: experimental data; — :density Redlich-Kister model

The calculated excess molar volume (V^E) of the binary mixture (virgin coconut oil + ethanol) at 323 K is illustrated in Figure 4.4. The V^E values were consistently negative across all solvent ratios. This trend indicated that the molecules in the mixed-solvent are packed closer than expected in an ideal mixture. Such behavior typically arises when intermolecular forces between the mixed-solvent are strong, such as hydrogen bonding and other attractive interactions. The most intense interaction was observed around x_1=0.6, corresponding to the highest xanthone solubility in the mixed-solvent.

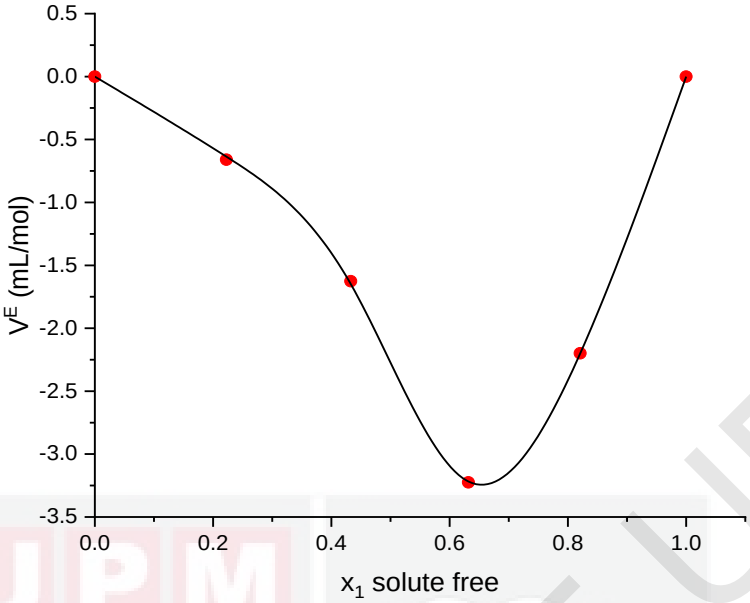

Figure 4.4 : Excess molar volume (V^E) of virgin coconut oil (VCO) + ethanol binary mixture at 323.15 K. Markers: experimental conditions; solid curve (calculated using Redlich-Kister model; x_1 represents volume fraction of VCO

4.3 Extraction Xanthone from Mangosteen Pericarp

Table 4.1 presents the results of xanthone extraction from mangsteen pericarp with and without ultrasound assistance for 15 min of extraction period. In the absence of ultrasound assistance, the xanthone concentration was the lowest for VCO (2.08 mg/mL), followed by VCO-ethanol (3.53 mg/mL) and ethanol (4.73 mg/mL). Using ethanol as the control, the addition of 40% ethanol into VCO increased the effectiveness of VCO as a solvent by up to 70%, resulting in a 57% enhancement in xanthone recovery. As shown in Figure 4.2, adding 40% ethanol to the VCO reduced the viscosity of the solvent from 35.5 mPas to 10 mPas. The increase in mass transfer efficiency caused by viscosity reduction has an effect on extraction efficiency in short extraction time. Additionally, the polarity of the solvent changed from non-polar (VCO) to slightly polar when ethanol was added.

When ultrasound was applied, the concentration of xanthone increased for VCO-based solvents, as shown in Table 4.1. Specifically, for VCO, the application of ultrasound enhanced the solvent's effectiveness by up to 64%, making it the most energy-efficient method for extracting xanthone from mangosteen pericarp, compared to the use of VCO-ethanol and ethanol alone. As the extraction period approached 15 minutes, the temperature in the VCO solvent was recorded at 342.25 K (17 W), 358.05 K (21 W), and 372.55 K (26 W), which were the highest temperatures compared to those achieved with the other solvents. This increase in temperature facilitates better mass transfer and reduces the viscosity of VCO, aiding in the extraction process and resulting in the highest energy efficiency among the solvents used in this study.

Ultrasound improved the solvent effectiveness of VCO-ethanol by 30% for all ultrasound treatments, making it as effective as ethanol. In terms of xanthone recovery, the application of ultrasound in VCO-based solvents markedly improved xanthone recovery, showing up to 62% recovery at 26 W ultrasound treatment.

The extraction profiles of xanthone from mangosteen pericarp are illustrated in Figure 4.5. The concentration of xanthone increased linearly over time (duration of 25 min) with the assistance of ultrasound in all extraction systems. The concentration of xanthone was influenced by both extraction time and power of ultrasound. Observations revealed that both extraction time and power of ultrasound had a positive impact on xanthone concentration. Prolonging the extraction time accumulated heat in the extraction system,

leading to an increase in xanthone concentration (Table 4.5). The amplitude directly affects the effective power output by the ultrasound generator, intensifying ultrasound cavitation, enhancing mangosteen particle vibration and crushing, and elevating the extraction system's temperature.

The discrepancy may arise from the complex interactions between the matrix and the solvents. Generally, extracting natural products involves a multifaceted process where variables such as solvent type, sample characteristics, extraction power, concentration, temperature, duration, and equipment all influence the results. Research indicates that flavonoids, due to their polarity, are more efficiently extracted with organic solvents like methanol. However, there is growing interest in using non-toxic and biodegradable alternatives like ethanol, which can minimize the environmental impact of organic solvents while delivering comparable or even superior performance (Fu et al. 2020). On the other hand, viscous solutions such as oils can amplify the effects of ultrasound waves but also impede their propagation and the mechanical effects of cavitation on the sample (Chaves et al. 2020). Consequently, the components in mangosteen pericarp may interact differently with pure ethanol versus a VCO-ethanol mixture, which could affect the availability and extraction efficiency of xanthones.

Table 4.3 : Extraction of xanthone from mangosteen pericarp

	Concentration of xanthone (mg/mL)				Solvent effectiveness				Energy effectiveness				Xanthone recovery			
Solvent	Ultrasound treatment															
	0 W	17 W	21 W	26 W	0 W	17 W	21 W	26 W	0 W	17 W	21 W	26 W	0 W	17 W	21 W	26 W
VCO	2.08	2.71	2.80	2.93	0.54	0.72	0.71	0.70	1.00	1.30	1.35	1.41	0.34	0.44	0.46	0.48
VCO-ethanol	3.53	3.61	3.72	3.84	0.93	0.97	0.95	0.92	1.00	1.02	1.05	1.09	0.57	0.59	0.60	0.62
Ethanol	3.81[a]	3.74	3.92	4.19	1.00	1.00	1.00	1.00	1.00	0.98	1.03	1.10	0.62	0.61	0.64	0.68

Note: VCO=virgin coconut oil; VCO: ethanol=6:4; extraction time=15 min; extraction without ultrasound treatment: 334.55 K; extraction with ultrasound treatment: temperature profiles are shown in Figure S9; solvent effectiveness was compared to ethanol; energy effectiveness was compared to 0 W; xanthone recovery was compared to concentration of xanthone extracted with ethanol for 800 min (6.16 mg/mL)

a: The pericarp of mangosteen were percolated by ethanol at room temperature for 20 h (Pothitirat et al. 2010).

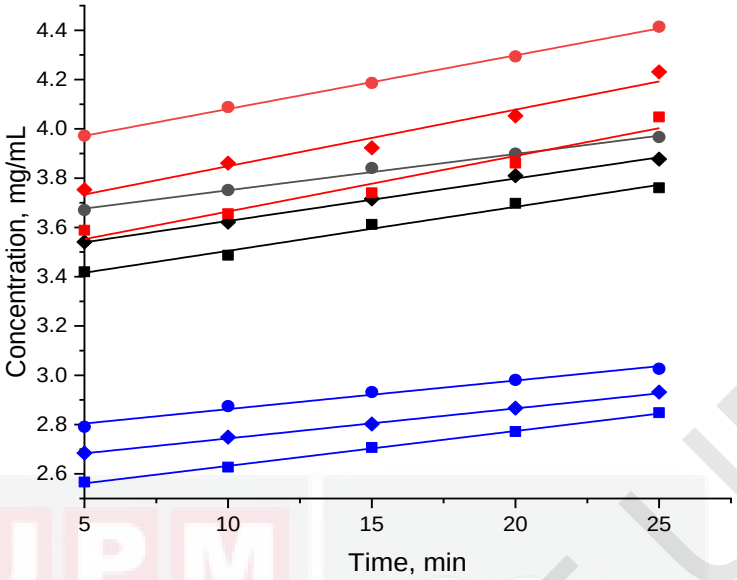

Figure 4.5 : Concentration of xanthone extracted from mangosteen pericarp by three different solvents at ultrasound intensity of 17 W, 21 W and 26 W. Red: ethanol, blue: virgin coconut oil (VCO), black: VCO: ethanol=6:4 (volume fraction) mixed-solvent. ■: 17 W, ◆: 21 W, ●:26 W. Marker: experimental data; solid line: Peleg's model

4.4 Ultrasound Assisted Extraction Kinetic Model

Tables 4.4-4.6 present the yields of xanthone extracted from mangosteen pericarp using ultrasound with three different solvents (ethanol, virgin coconut oil (VCO), and their mixture) fitted to three different extraction models. The extraction models include Peleg's model, the pseudo-second-order kinetic model prototype (type 1), and its improved model (type 2). The data were fitted with Peleg and improved pseudo-second-order kinetic models with R^2 more than 0.99 as shown in Figure 4.6. These models could be used for scaling up the extraction process and ensuring quality control.

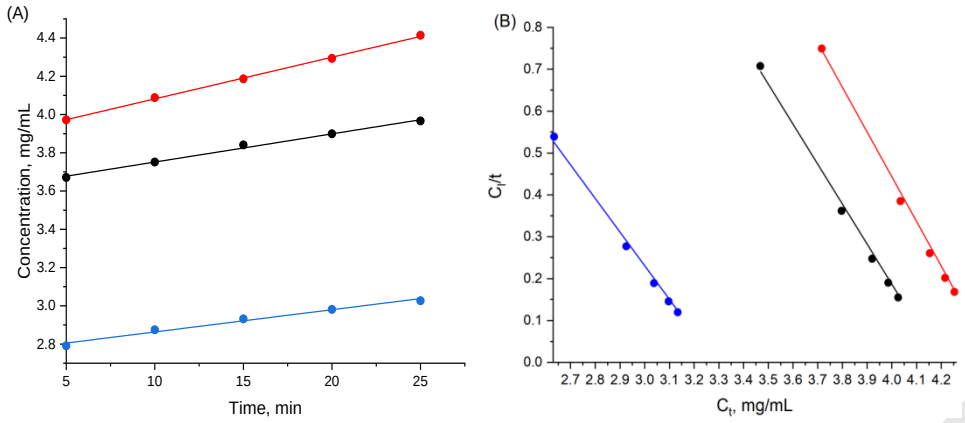

Figure 4.6 : Kinetics model of ultrasound-assisted extraction of xanthone from mangosteen pericarp at ultrasound intensity of 26 W. Marker: experimental values; Solid line: A): Peleg's model; (B): pseudo-second-order kinetic model type 2. Blue (virgin coconut oil), red (ethanol) and black (VCO: ethanol, 6: 4)

Table 4.4 : Kinetic model of ultrasound-assisted extraction (UAE) of xanthone with mixed-solvent (virgin coconut oil (VCO): ethanol volume ratio=6:4) at different intensities (C_0 and C_e, mg/mL; k_1, mL min/mg; k_2, mL /mg; K, mL/(mg min))

Model	Ultrasound Intensity (W)	Constants	R^2
Peleg' s	17	C_0=3.328 k_1=27.742 k_2=28.351	0.9874
	21	C_0=3.455 k_1=28.689 k_2=29.324	0.9971
	26	C_0=3.604 k_1=28.542 k_2=39.215	0.9939
pseudo-second-order kinetic model type 1	17	C_e=3.933 K=0.211	0.9364
	21	C_e=4.049 K=0.21	0.9201
	26	C_e=4.162 K=0.195	0.8582
pseudo-second-order kinetic model type 2	17	C_e=4.032 K=0.257	0.9966
	21	C_e=4.195 K=0.228	0.9959
	26	C_e=4.315 K=0.244	0.9962

Table 4.5 : Kinetic model of ultrasound-assisted extraction of xanthone with ethanol at different intensities (C_0 and C_e, mg/mL; k_1, mL min/mg; k_2, mL /mg; K, mL/(mg min))

Model	Ultrasound Intensity (W)	Constants	R^2
Peleg's	17	C_0=3.441 K_1=23.254 K_2=21.194	0.9568
	21	C_0=3.62 K_1=22.412 K_2=21.185	0.9686
	26	C_0=3.864 K_1=23.931 K_2=22.047	0.9989
pseudo-second-order kinetic model type 1	17	C_e=4.19 K=0.203	0.6959
	21	C_e=4.404 K=0.1791	0.7492
	26	C_e=4.573 K=0.204	0.8420
pseudo-second-order kinetic model type 2	17	C_e=4.173 K=0.274	0.9970
	21	C_e=4.412 K=0.242	0.9971
	26	C_e=4.605 K=0.247	0.9981

Table 4.6 : Kinetic model of ultrasound-assisted extraction of xanthone with virgin coconut oil (VCO) at different intensities (C_0 and C_e, mg/mL; k_1, mL min/mg; k_2, mL /mg; K, mL/(mg min))

Model	Ultrasound Intensity (W)	Constants	R^2
Peleg's	17	C_0=2.492 K_1=35.406 K_2=35.307	0.998
	21	C_0=2.623 K_1=42.019 K_2=40.087	0.999
	26	C_0=2.748 K_1=44.891 K_2=41.142	0.983
pseudo-second-order kinetic model type 1	17	C_e=3.022 K=0.207	0.8687
	21	C_e=3.134 K=0.187	0.7354
	26	C_e=3.212 K=0.213	0.7510
pseudo-second-order kinetic model type 2	17	C_e=3.119 K=0.276	0.9944
	21	C_e=3.291 K=0.244	0.9926
	26	C_e=3.374 K=0.262	0.9946

4.5 Statistical Analysis

As shown in Table 4.7, parameter A represents the extraction time (min), B represents the ultrasound intensity (W), and C represents the ratio of virgin coconut oil (VCO) in the mixed-solvent. The independent parameters A, B, and C, as well as the interaction parameters AC, BC, and the quadratic parameter C^2, were significant model items. These parameters collectively influence the extraction efficiency and yield of xanthone from mangosteen pericarp. The significance of the interaction and quadratic parameters highlighted the complex nature of the extraction process, where the combined effects of extraction time, ultrasound intensity, and solvent composition interact to determine the overall effectiveness.

Equation 4.1 shows the regression of xanthone concentration to experimental parameters. The positive regression coefficient of A, B and C showed that an increase in extraction time, ultrasound intensity and solvent ratio led to an increase in xanthone yield. On the other hand, the negative regression coefficients of AC, BC and C^2 indicated that the interactions between extraction time and solvent ratio, ultrasound intensity and solvent ratio, and the quadratic effect of solvent ratio, respectively, had a diminishing effect on xanthone yield. This suggests that while increasing each of these parameters individually can enhance yield, their combined or excessive influence may lead to inefficiencies or suboptimal extraction conditions. Che Sulaiman et al. found similar results when extracting phenolic compounds in *Clinacanthus nutans* Lindau leaves with different ratios of ethanol/water. Extending the extraction time at 80°C can actually decrease the extraction rate because prolonged

exposure to high temperatures can result in oxidation and degradation of the target compounds. (Che Sulaiman et al. 2017). Xu et al.'s study on the extraction of lycopene from red grapefruit using ultrasound-assisted mixed solvents revealed that increasing the ultrasound intensity from 605 W/cm² to 1089 W/cm² significantly reduced the yield of lycopene ($p < 0.05$). This observation suggests that ultrasound intensity is crucial for extracting all-trans lycopene. As ultrasound intensity increased from 0 W/cm² to 605 W/cm², the number of cavitation microbubbles in the liquid grew, and their collapse rate accelerated, which enhanced the disruption of tissue cell walls and promoted faster diffusion of lycopene. However, when the intensity exceeded 605 W/cm², the cavitation bubbles may have become too large to collapse efficiently or collapsed more slowly, reducing the effectiveness of cavitation. Additionally, excessive bubble formation at high intensities can obstruct the propagation of ultrasound waves or cause scattering, further diminishing extraction efficiency (Xu et al. 2013). This result is consistent with the calculation result that B^2 (the quadratic effect of ultrasound intensity) has no significant effect on the extraction rate of xanthone.

Table 4.7 : Estimation regression coefficient and analysis of variance (ANOVA) for the investigated parameters

Factor	Regression coefficient	T-Value	p-Value	Remarks
Constant	2.467	13.78	<0.001	Significant
A (Time, min)	0.02451	6.25	<0.001	Significant
B (Ultrasound intensity, W)	0.0646	3.95	<0.001	Significant
C (Solvent ratio)	1.2976	20.08	<0.001	Significant
AB	-0.000237	-1.75	0.088	Not significant
AC	-0.00976	-8.05	<0.001	Significant
BC	-0.02274	-9.77	<0.001	Significant
A^2	0.000099	1.18	0.246	Not significant
B^2	-0.000396	-1.06	0.297	Not significant
C^2	-1.8077	-57.69	<0.001	Significant
R^2	0.9985	Adjusted R^2	0.9981	

The regression coefficient reflects the impact of each parameter on the experimental response, with the coefficient's size indicating the weight of its influence and the sign indicating an increase or decrease. The regression coefficient for A is positive, and the regression coefficient for C is also positive. In this context, a positive regression coefficient for A and C means that an increase in extraction time and solvent ratio leads to an increase in xanthone yield. On the other hand, the regression coefficients for AC and BC are negative, and the regression coefficient for C^2 is also negative. The values of the regression coefficients provide insights into the magnitude of the effect on the dependent variable.

For parameter A, increasing 1unit results in 0.02451 times increase in xanthone concentration, while increasing C by 1 unit leads to 1.2976 times decrease in xanthone concentration. The empirical model for the xanthone yield parameter can be expressed as follows:

$$Concentration = 2.467 + 0.02451A + 0.0646B + 1.2976C - 0.00976AC - 0.002274BC - 1.8077C^2 \quad (4.1)$$

Where A is the extraction time, B is the amplitude percentage, and C is the solvent ratio.

Figure 4.7 illustrates a response surface plot derived from the fitted model, where one variable is maintained at a moderate level (time=15 min, ultrasound intensity=21 W, and virgin coconut oil (VCO) ratio=0.6), while the other two variables are varied within the experimental range. Figure 4.7 (A) presents

plots of time and intensity variables with intermediate VCO proportion levels. According to Table 4.10, time and intensity are deemed significant ($p < 0.001$). The increase in extraction time, without constant temperature conditions, intensifies the ultrasound waves' crushing and puncturing effect on mangosteen pericarp particles, enhancing the contact area between the solvent and the solid. Consequently, this leads to an increased diffusion rate of the solvent, resulting in a higher yield of xanthone.

Figures 4-7 (B) and (C) depict that mixed-solvents exhibit a higher extraction rate for xanthone in ultrasound-assisted extraction (UAE) compared to pure VCO. This is attributed to the lower viscosity and the addition of ethanol, which increases the hydrogen bond donating capacity of the solvent and adjusts its polarity. As indicated in table 4-10, the solvent ratio was a significant parameter ($p < 0.001$).

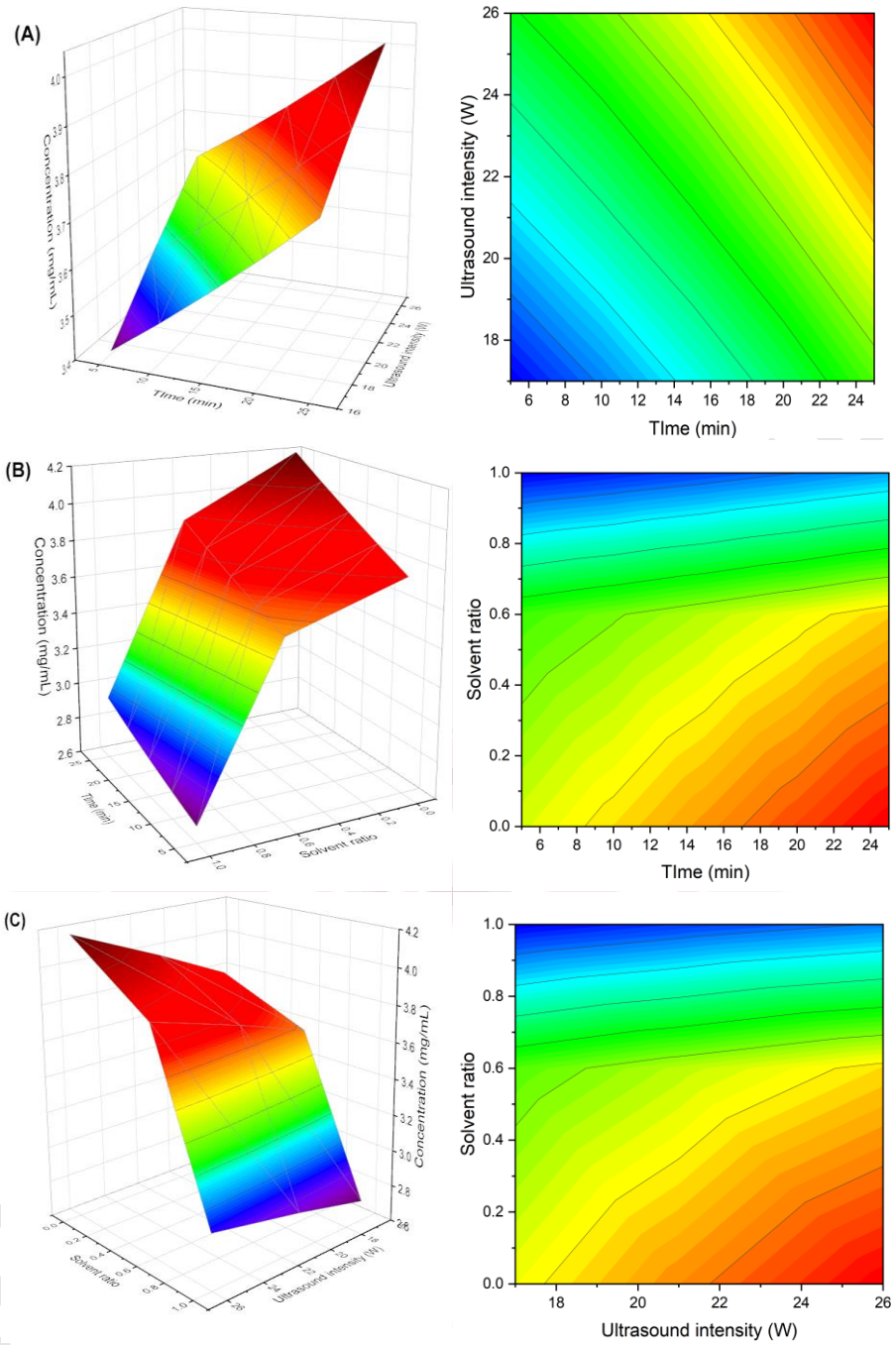

Figure 4.7 : Response surface plots representing the effects of (A) time and ultrasound intensity, (B) time and solvent ratio, and (C) ultrasound intensity and solvent ratio on the yield of xanthone

CHAPTER 5

SUMMARY, CONCLUSION AND RECOMMENDATIONS FOR FUTURE RESEARCH

5.1 Summary

The research indicates that the solubility of xanthone is significantly enhanced in a mixed-solvent of virgin coconut oil (VCO) and ethanol, reaching its peak at a VCO volume fraction of 0.6. This heightened solubility is attributed to lower viscosity, higher density, and increased hydrogen bond donors in the solvent.

Ultrasound assisted extraction (UAE) utilizing a 26 W ultrasound intensity and a 25 min extraction time proved highly effective, outperforming other extraction methods. The addition of ethanol as a co-solvent further improved the xanthone extraction rate from VCO.

The study suggests that mixed-solvents, combining VCO with low-viscosity organic solvents rich in hydrogen bond donors like ethanol, show promise as alternatives to traditional solvents for xanthone dissolution. Moreover, incorporating ultrasound-assisted extraction technology enhances overall extraction efficiency in the process of obtaining xanthone from mangosteen pericarp.

5.2 Conclusion

This experiment highlights that the solubility of xanthone is notably elevated in a mixed-solvent of virgin coconut oil and ethanol, with the optimum solubility

achieved at a 0.6 volume ratio of virgin coconut oil. The impact of the interaction between xanthone and the solvent on the solubility was confirmed through the analysis of the density of the solvent and the excess molar volume of the dissolved system.

Ultrasound-assisted extraction experiments demonstrated a positive correlation between ultrasound intensity, extraction time, and xanthone concentration. Importantly, the mixed-solvent exhibited significantly improved xanthone extraction capabilities compared to using pure virgin coconut oil. These findings underscore the potential of mixed-solvents, particularly when paired with ultrasound-assisted extraction, for enhanced xanthone extraction efficiency from mangosteen pericarp.

5.3 Recommendations

Certainly, further experiments would be valuable to refine the choice of cosolvent and achieve a stable miscible state with virgin coconut oil at room temperature. It's crucial to explore different combinations and ratios of cosolvents to find the most effective and stable solution for improved xanthone solubility.

Additionally, a deeper investigation into the mechanism through which the mixed-solvent enhances xanthone solubility would provide valuable insights. This could involve more detailed analyses using advanced techniques to understand the specific interactions, molecular changes, and the role of each component in the mixed-solvent. Techniques such as molecular dynamics

simulations or advanced spectroscopy methods may be employed for a more in-depth understanding of the molecular-level processes occurring during the solubility enhancement.

REFERENCES

Abdkarimi, F. (2021). Solubility measurement and thermodynamic modeling of sertraline hydrochloride and clopidogrel bisulfate in deep eutectic solvent of choline chloride and malonic acid. Journal of Molecular Liquids. 344, 117940.

Agarwal, C. (2018). Ultrasound-Assisted Extraction of Cannabinoids from Cannabis Sativa L. Optimized by Response Surface Methodology. Journal of Food Science. 83(3), 700-710.

Alam, M. S. (2018). The density, dynamic viscosity and kinematic viscosity of protic polar solvents (pure and mixed systems) studies: A theoretical insight of thermophysical properties. Journal of Molecular Liquids. 251, 458-469.

Bao, R. (2023). A comparative evaluation of low-field and high-field NMR untargeted analysis: Authentication of virgin coconut oil adulterated with refined coconut oil as a case study. Analytica Chimica Acta. 1273, 341537.

Çalış, İ. (2023). Comparative phytochemical studies on the roots of Polygala azizsancarii and P. peshmenii and neuroprotective activities of the two xanthones. Phytochemistry. 210, 113650.

Chaves, J. O. (2020). Extraction of Flavonoids From Natural Sources Using Modern Techniques. Frontiers in Chemistry. 8.

Che Sulaiman, I. S. (2017). Effects of temperature, time, and solvent ratio on the extraction of phenolic compounds and the anti-radical activity of Clinacanthus nutans Lindau leaves by response surface methodology. Chemistry Central Journal. 11(1), 54.

Cheng, S. (2022). Solubility determination and dissolution thermodynamic properties of dodecanedioic acid in binary-mixed solvents from T = (288.15–328.15) K. The Journal of Chemical Thermodynamics. 166, 106686.

Cortés, J. C. (2023). Statistical analysis of randomized pseudo-first/second order kinetic models. Application to study the adsorption on cadmium ions onto tree fern. Chemometrics and Intelligent Laboratory Systems. 104910.

De Laet, E. (2024). Influence of ultrasound-assisted extraction on the pectin extraction yield and structural characteristics: a case study on carrot pomace (Daucus carota). Food and Bioproducts Processing.

Du, C. (2023). Effect of alkali and alkaline earth metals on the liquefaction of lignocellulosic model compounds to prepare bio-oil in ethanol solvent. Energy. 278, 127614.

Fu, X. (2020). Sono-physical and sono-chemical effects of ultrasound: Primary applications in extraction and freezing operations and influence on food components. Ultrasonics Sonochemistry. 60, 104726.

Gupta, S. (2016). Elucidation of intriguing methanol-dichloromethane binary solvent mixture: Synergistic effect, analytical modeling, NMR and photo-induced electron transfer studies. Journal of Molecular Liquids. 223, 274-282.

Ha, E.-S. (2019). Solubility and modeling of telmisartan in binary solvent mixtures of dichloromethane and (methanol, ethanol, n-propanol, or n-butanol) and its application to the preparation of nanoparticles using the supercritical antisolvent technique. Journal of Molecular Liquids. 295, 111719.

Huang, Y.-T. (2018). A Study on the Pseudo-Second-Order Kinetic Equation for the Adsorption of Methylene Blue onto Nitric Acid-Treated Rice Husk: Comparison of Linear Methods. International Journal of Scientific and Research Publications (IJSRP). 8.

Izza, H. F. (2023). Performance of microwave-assisted extraction of proanthocyanidins from red sorghum grain in various power and citric acid concentration. Journal of the Saudi Society of Agricultural Sciences.

Jeong, J.-S. (2022). Measurement and correlation of solubility of rivaroxaban in dichloromethane and primary alcohol binary solvent mixtures at different temperatures. Journal of Molecular Liquids. 357, 119064.

Jiang, X. (2014). Selecting water-alcohol mixed solvent for synthesis of polydopamine nano-spheres using solubility parameter. scientific reports.

Kalick, L. S. (2023). Mangosteen for malignancy prevention and intervention: Current evidence, molecular mechanisms, and future perspectives. Pharmacological Research. 188, 106630.

Khursheed, T. (2024). Ultrasound-assisted solvent extraction of phenolics, flavonoids, and major triterpenoids from Centella asiatica leaves: A comparative study. Ultrasonics Sonochemistry. 107091.

Kok, S. L. (2021). Role of virgin coconut oil (VCO) as co-extractant for obtaining xanthones from mangosteen (Garcinia mangostana) pericarp with supercritical carbon dioxide extraction. The Journal of Supercritical Fluids. 176, 105305.

Kusmayadi, A. (2018). The effect of solvents and extraction time on total xanthone and antioxidant yields of mangosteen peel (Garcinia mangostana L.) extract. Drug Invention Today. 10, 2572-2576.

Lee, S.-K. (2023). Synergistic solvation effect and modeling of itraconazole solubility in eight binary mixtures (dichloromethane and chloroform + primary alcohol) at the range of 288.15 K to 308.15 K. The Journal of Chemical Thermodynamics. 185, 107115.

Lee, W. J. (2019). Supercritical carbon dioxide extraction of α-mangostin from mangosteen pericarp with virgin coconut oil as co-extractant and in-vitro bio-accessibility measurement. Process Biochemistry. 87.

Li, L. (2024). Extraction of Isobutanol from Aqueous Solution by Four Solvents: Liquid–Liquid Phase Equilibrium Measurements and Thermodynamic Modeling Studies. Journal of Chemical & Engineering Data. 69(7), 2596-2605.

Mazaher Haji Agha, E. (2020). Solubility and thermodynamic properties of mesalazine in {2-propanol + water} mixtures at various temperatures. Journal of Molecular Liquids. 301, 112474.

Mihalovits, M. (2022). Determination of the Hansen solubility parameters from solubility data using an improved evaluation approach, the concentric spheroids method. Journal of Molecular Liquids. 364, 119911.

Milićević, N. (2021). Kinetic modelling of ultrasound-assisted extraction of phenolics from cereal brans. Ultrasonics Sonochemistry. 79, 105761.

Mohammad, N. A. (2019). Optimization of the antioxidant-rich xanthone extract from mangosteen (Garcinia mangostana L.) pericarp via microwave-assisted extraction. Heliyon. 5(10), e02571.

Morini, M. A. (2020). Interaction of hydroxy-xanthones with phosphatidylcholines: The effector decreases compressibility and increases the fluidity of membranes. Chemistry and Physics of Lipids. 231.

Moussout, H. (2018). Critical of linear and nonlinear equations of pseudo-first order and pseudo-second order kinetic models. Karbala International Journal of Modern Science. 4(2), 244-254.

Nasrullah, A. (2019). Mangosteen peel waste as a sustainable precursor for high surface area mesoporous activated carbon: Characterization and application for methylene blue removal. Journal of Cleaner Production. 211, 1190-1200.

Phyo, Y. Z. (2021). Chiral derivatives of xanthones and benzophenones: Synthesis, enantioseparation, molecular docking, and tumor cell growth inhibition studies. Chirality. 33(4), 153-166.

Pinto, M. (2021). molecules Review From Natural Products to New Synthetic Small Molecules: A Journey through the World of Xanthones. Molecules. 26.

Polok, K. (2022). Search for the origin of synergistic solvation in methanol/chloroform mixture using optical Kerr effect spectroscopy. Journal of Molecular Liquids. 345, 117013.

Pothitirat, W. (2010). Free radical scavenging and anti-acne activities of mangosteen fruit rind extracts prepared by different extraction methods. Pharmaceutical Biology. 48(2), 182-186.

Preston, J. A. (2024). Elucidating the Polymorphism of Xanthone: A Crystallization and Characterization Study. Crystal Growth & Design. 24(8), 3256-3268.

Pujirahayu, N. (2015). Antibacterial activity of oil extract of trigona propolis. International Journal of Pharmacy and Pharmaceutical Sciences. 7(6), 419-422.

Qiu, J. (2019). Synergistic Solvation Effects: Enhanced Compound Solubility Using Binary Solvent Mixtures. Organic Process Research & Development. 23(7), 1343-1351.

Rana, M. N. (2020). Xanthones protects lead-induced chronic kidney disease (CKD) via activating Nrf-2 and modulating NF-kB, MAPK pathway. Biochemistry and Biophysics Reports. 21, 100718.

Regazzoni, A. E. (2020). Adsorption kinetics at solid/aqueous solution interfaces: On the boundaries of the pseudo-second order rate equation. Colloids and Surfaces A: Physicochemical and Engineering Aspects. 585, 124093.

Ridwan, R. D. (2021). A study of the mucoadhesive patches loaded with mangosteen peel extract in periodontitis. Journal of Taibah University Medical Sciences. 16(6), 864-869.

Shafaei, S. M. (2016). Analysis of water absorption of bean and chickpea during soaking using Peleg model. Journal of the Saudi Society of Agricultural Sciences. 15(2), 135-144.

Suksamran, N. (2022). Mangosteen vinegar from Garcinia mangostana: quality improvement and antioxidant properties. Heliyon. 8(12), e11943.

Tang, Z. (2023). Ultrasound-assisted extraction, analysis and antioxidant activity of polysaccharide from the rinds of Garcinia mangostana L. Ultrasonics Sonochemistry. 97, 106474.

Vargas-Campos, L. (2023). Study of the dextrose equivalent of maltodextrins in electrospinning using an ethanol/water mixture as the electrospinning solvent. Food Hydrocolloids. 139, 108498.

Vo, T. P. (2023). Green extraction of total phenolic and flavonoid contents from mangosteen (Garcinia mangostana L) rind using natural deep eutectic solvents. Heliyon. 9(4), e14884.

Wani, T. A. (2017). Study of binding interaction of rivaroxaban with bovine serum albumin using multi-spectroscopic and molecular docking approach. Chemistry Central Journal. 11(1), 134.

Xu, Y. (2013). Effects of various factors of ultrasonic treatment on the extraction yield of all-trans-lycopene from red grapefruit (Citrus paradise Macf.). Ultrasonics Sonochemistry. 20(4), 1026-1032.

Yan, J. (2023). Extraction desulfurization with mixed solvents of organic solvent + organic solvent or deep eutectic solvent as extractants: Liquid-liquid equilibrium experiments and molecular dynamics simulations. Fluid Phase Equilibria. 565.

Yara-Varón, E. (2017). Vegetable Oils as Alternative Solvents for Green Oleo-Extraction, Purification and Formulation of Food and Natural Products. Molecules. 22(9).

Żelaszczyk, D. (2024). Antibacterial and antibiofilm agents in the group of xanthone derivatives with piperazine moiety active against drug-resistant Helicobacter pylori strains. Bioorganic Chemistry. 153, 107755.

Zhang, Y. (2021). Machine learning bioactive compound solubilities in supercritical carbon dioxide. Chemical Physics. 550, 111299.

Zhao, J. (2023). Solid-liquid phase equilibrium of 2, 4-epibrassinolide in binary mixed solvents: Solubility determination, model correlation, preferential solvation and thermodynamic properties. The Journal of Chemical Thermodynamics. 184, 107066.

Zheng, Y.-Z. (2021). The important role of benzylic CH bond in the antioxidant behaviours of the xanthones. Journal of Food Composition and Analysis. 103, 104082.

APPENDICES

Table S1 : Calibration curves of xanthone in different solvents (virgin coconut oil (VCO) and ethanol)

VCO volume fraction	Slope	Intercept	R^2
0	100.84	0.0439	0.9999
0.1	86.12	-0.0519	0.9993
0.2	68.28	0.0391	0.9997
0.3	55.72	0.0067	0.9961
0.4	46.64	0.0746	0.9989
0.5	40.44	0.0181	0.9997
0.6	34.8	0.0606	0.9999
0.7	42.24	0.032	0.9997
0.8	48.32	0.0358	0.9985
0.9	50.08	0.0408	0.9988
1	75.4	-0.0283	0.9992

The solubility of xanthone was calculated using the following formula.

$$x = 1 + \left[\frac{T(a-i)}{1000 \times S \times M_{xan}} \times \frac{1}{\frac{m_v}{M_v} + \frac{m_e}{M_e}}\right] \quad (1)$$

Where x is the mole fraction of xanthone, T represents the dilution factor when measuring absorbance, a represents the absorbance value, i is the intercept value of the calibration curve, S represents the slope of the calibration curve, M is the molar mass, m is the mass (xan, v and e stand for xanthone, VCO and ethanol respectively).

Table S2 : Experimental mass fraction solubility of xanthone in virgin coconut oil + ethanol binary-mixed-solvents from 303.15 K to 323.15 K

VCO v/v solute free	Absorbance	slope	intercept	Mass xanthone in 1mL solution, g	Mass solvents in 1 mL solution, g	Mass fraction of xanthone
303.15K						
0.000	0.491	100.84	0.0439	0.0089	0.7793	0.0113
0.113	0.362	86.12	-0.0519	0.0096	0.7913	0.0120
0.222	0.399	68.28	0.0391	0.0105	0.8049	0.0129
0.329	0.34	55.72	0.0067	0.0120	0.8190	0.0144
0.433	0.405	46.64	0.0746	0.0142	0.8353	0.0167
0.534	0.371	40.44	0.0181	0.0175	0.8550	0.0200
0.632	0.449	34.8	0.0606	0.0223	0.8709	0.0250
0.728	0.383	42.24	0.032	0.0166	0.8800	0.0185
0.821	0.362	48.32	0.0358	0.0135	0.8884	0.0150
0.912	0.333	50.08	0.0408	0.0117	0.9026	0.0128
1.000	0.377	75.4	-0.0283	0.0108	0.9159	0.0116
308.15K						
0.000	0.512	100.84	0.0439	0.0093	0.7755	0.0118
0.113	0.386	86.12	-0.0519	0.0102	0.7876	0.0127
0.222	0.42	68.28	0.0391	0.0112	0.8012	0.0137
0.329	0.359	55.72	0.0067	0.0126	0.8153	0.0153
0.433	0.428	46.64	0.0746	0.0152	0.8316	0.0179
0.534	0.397	40.44	0.0181	0.0187	0.8513	0.0215
0.632	0.480	34.8	0.0606	0.0241	0.8672	0.0270
0.728	0.404	42.24	0.032	0.0176	0.8764	0.0197
0.821	0.376	48.32	0.0358	0.0141	0.8846	0.0157
0.912	0.345	50.08	0.0408	0.0121	0.8988	0.0133
1.000	0.391	75.4	-0.0283	0.0111	0.9122	0.0120
313.15K						
0.000	0.532	100.84	0.0439	0.0097	0.7717	0.0124
0.113	0.41	86.12	-0.0519	0.0107	0.7840	0.0135
0.222	0.441	68.28	0.0391	0.0118	0.7975	0.0145
0.329	0.378	55.72	0.0067	0.0133	0.8116	0.0162
0.433	0.451	46.64	0.0746	0.0161	0.8279	0.0191

0.534	0.424	40.44	0.0181	0.0201	0.8476	0.0231
0.632	0.511	34.8	0.0606	0.0259	0.8635	0.0291
0.728	0.435	42.24	0.032	0.0191	0.8728	0.0214
0.821	0.391	48.32	0.0358	0.0147	0.8808	0.0164
0.912	0.356	50.08	0.0408	0.0126	0.8950	0.0139
1.000	0.405	75.4	-0.0283	0.0115	0.9086	0.0125
323.15K						
0.000	0.573	100.84	0.0439	0.0105	0.7640	0.0135
0.113	0.443	86.12	-0.0519	0.0115	0.7768	0.0146
0.222	0.475	68.28	0.0391	0.0128	0.7901	0.0159
0.329	0.415	55.72	0.0067	0.0147	0.8043	0.0179
0.433	0.496	46.64	0.0746	0.0181	0.8206	0.0215
0.534	0.476	40.44	0.0181	0.0226	0.8403	0.0262
0.632	0.573	34.8	0.0606	0.0294	0.8562	0.0333
0.728	0.478	42.24	0.032	0.0211	0.8656	0.0238
0.821	0.42	48.32	0.0358	0.0159	0.8733	0.0179
0.912	0.379	50.08	0.0408	0.0135	0.8875	0.0150
1.000	0.433	75.4	-0.0283	0.0122	0.9013	0.0134

Table S3 : Experimental mass fraction solubility of xanthone in virgin coconut oil + ethanol binary-mixed-solvents from 303.15 K to 323.15 K

x_1	303.15 K	308.15 K	313.15 K	323.15 K
0.000	7.2×10^{-5}	3.2×10^{-5}	5×10^{-5}	3.2×10^{-5}
0.113	8×10^{-6}	1.8×10^{-5}	8×10^{-6}	8×10^{-6}
0.222	1.8×10^{-5}	8×10^{-6}	3.2×10^{-5}	1.8×10^{-5}
0.329	8×10^{-6}	5×10^{-5}	1.8×10^{-5}	1.8×10^{-5}
0.433	8×10^{-6}	5×10^{-5}	1.8×10^{-5}	1.8×10^{-5}
0.534	5×10^{-5}	3.2×10^{-5}	1.8×10^{-5}	5×10^{-5}
0.632	1.8×10^{-5}	1.8×10^{-5}	3.2×10^{-5}	5×10^{-5}
0.728	3.2×10^{-5}	8×10^{-6}	1.8×10^{-5}	2×10^{-6}
0.821	1.8×10^{-5}	8×10^{-6}	8×10^{-6}	8×10^{-6}
0.912	8×10^{-6}	1.8×10^{-5}	3.2×10^{-5}	1.8×10^{-5}
1.000	2×10^{-6}	1.8×10^{-5}	1.8×10^{-5}	8×10^{-6}

Table S4 : The density of the mixture of virgin coconut oil (VCO) and ethanol at 2 different temperatures

Volume fraction of VCO	Density, g/mL	
	308.15K	323.15K
0.0	0.7755	0.7640
0.1	0.7876	0.7768
0.2	0.8012	0.7901
0.3	0.8153	0.8043
0.4	0.8316	0.8206
0.5	0.8513	0.8403
0.6	0.8672	0.8562
0.7	0.8764	0.8656
0.8	0.8846	0.8733
0.9	0.8988	0.8875
1.0	0.9122	0.9013

Table S5 : Calculation data of excess molar volume (V^E) of virgin coconut oil and ethanol mixed-solvent at 323.15K

Mole fraction of VCO	ρ_{id}, g/mL	ρ_{ex}, g/mL	ρ_{mix}, g/mL	V^E RK model	V^E,mL/mol
0.0000	0.7640	0.0000	0.7640	0.0000	0.0000
0.0148	0.7825	0.0073	0.7899	-0.6368	-0.6606
0.0385	0.8043	0.0165	0.8208	-1.6492	-1.6265
0.0827	0.8304	0.0257	0.8561	-3.2177	-3.2250
0.1938	0.8620	0.0113	0.8733	-2.1997	-2.1992
1.0000	0.9013	0.0000	0.9013	0.0000	0.0000

Table S6 : Redlich- Kister model for viscosity of virgin coconut oil and ethanol mixed-solvent 323.15K

Fitting parameter	Value
A_1	33.08601952
B_1	0.241832551

Table S7 : Redlich- Kister model for density and excess molar volume (V^E) of virgin coconut oil and ethanol mixed-solvent 323.15K

Fitting parameter	Value
A1	1.0593
B1	-0.0053
A2	1.0816
B2	-0.0071

The measured density values have been used to calculate excess molar volumes (V^E) by the following equation:

$$V^E = \frac{\sum_{i=1}^{n} x_i M_i}{\rho} - \sum_{i=1}^{n} \frac{x_i M_i}{\rho_i}$$ (Jiang et al. 2014)

where x_i represents the mole fraction of the pure component, M_i is the molar mass of the pure component, ρ is the density of the mixture, ρ_i denotes the density of each pure component, and n refers to the number of components present in the system.

Using the additive behavior approach, the ideal behavior of density is given in Eq. (2) as:

$$\rho_{id} = \frac{\sum x_i MW_i}{\sum \frac{x_i MW_i}{\rho_i}} \quad (2)$$

where MWi denotes the molecular weight of component i and xi represents the mole fraction of component i. illustrates the excess term using the Redlich-Kister (RK) expansion, which accounts for deviations from ideal density in a mixture of two components, A and B.

$$\rho_{ex} = x_A x_B \sum_{j=1}^{n} L_j (x_A - x_B)^{j-1} \quad (3)$$

where j specifies the order of the expansion, while L_j represents the j-th order binary interaction parameter between components A and B. This parameter exhibits a linear temperature dependence, as described by Eq. (4).

$$L_j = A_j + B_j T \quad (4)$$

Table S8 : Evaporation test of ethanol under sealed conditions

Group	1	2
Placement time	23h	21h
Initial weight, g	32.217	19.889
Final weight, g	32.209	19.882
Evaporation weight, g	0.008	0.007

Table S9 : Concentration (mg/mL) measured for mangosteen pericarp in virgin coconut oil (VCO), ethanol and mixed-solvent (VCO:ethanol=6:4 (v/v)) at different time and ultrasound intensity (W)

Solvent	Time(min)	Concentration (mg/mL) of xanthone		
		17W	21W	26W
VCO	5	2.567	2.685	2.791
	10	2.628	2.749	2.875
	15	2.707	2.802	2.932
	20	2.772	2.867	2.981
	25	2.848	2.932	3.027
Ethanol	5	3.588	3.754	3.972
	10	3.655	3.861	4.088
	15	3.740	3.923	4.187
	20	3.861	4.053	4.294
	25	4.048	4.231	4.414
Mixed-solvent	5	3.420	3.541	3.671
	10	3.487	3.622	3.752
	15	3.613	3.716	3.841
	20	3.698	3.810	3.900
	25	3.761	3.877	3.967

Table S10 : The final temperature of the mangosteen pericarp extraction system under different solvents, extraction times and ultrasound power

Solvent	Time(min)	Extraction temperature (℃) at 3 ultrasound Intensities		
		17W	21W	26W
VCO	5	47.1	60.7	75.2
	10	60.2	76.8	91.7
	15	69.1	84.9	99.4
	20	77.5	93.4	107.4
	25	81.9	97.6	111
Ethanol	5	32.1	38.9	43.6
	10	39.1	46.9	53.4
	15	42.6	50.3	61.7
	20	47.8	56.8	65.2
	25	49.3	59.3	68.9
Mixed-solvent	5	36.8	47.2	59
	10	42.4	53.6	65.2
	15	45.8	58.3	69.8
	20	49.3	60.1	71.9
	25	52.4	62.8	73.9

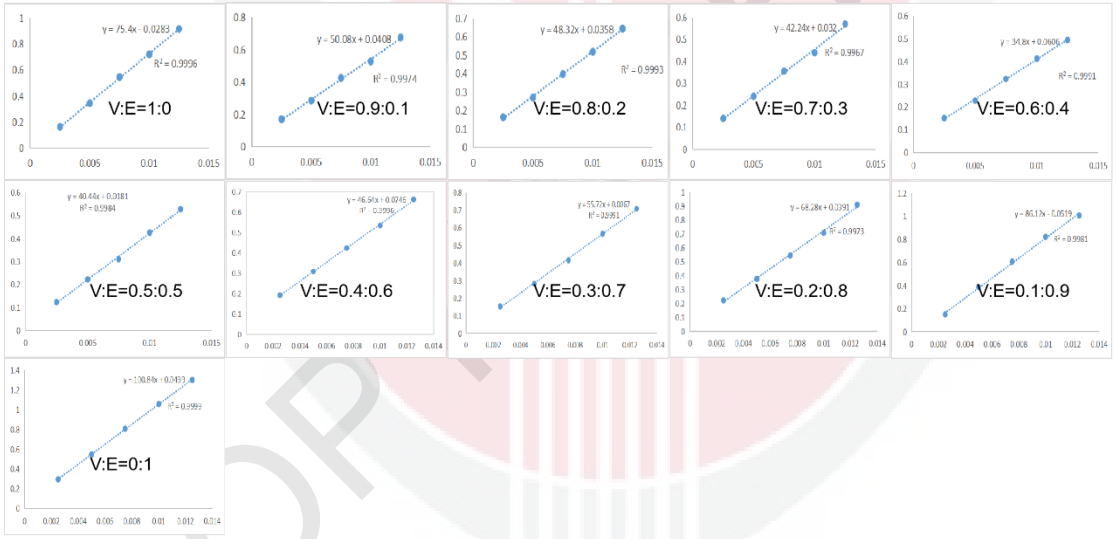

Figure S1 : UV-Vis spectrophotometry calibration cruve for different ratios of virgin coconut oil (VCO) and ethanol (V: VCO, E: ethanol)

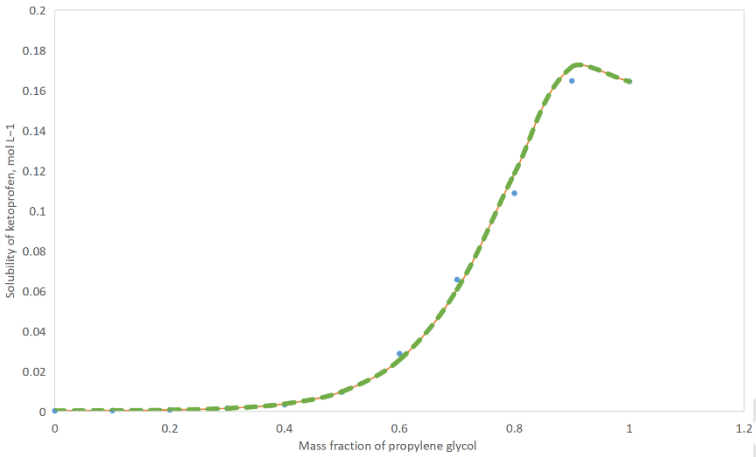

Figure S2 : Solubility of ketoprofen (3) in propylene glycol (1) + water (2) cosolvent mixtures. Marker: experimental data; Solid line—: the model predicted values in the original article; Breaking line-----: modified Jouyban-Acree model

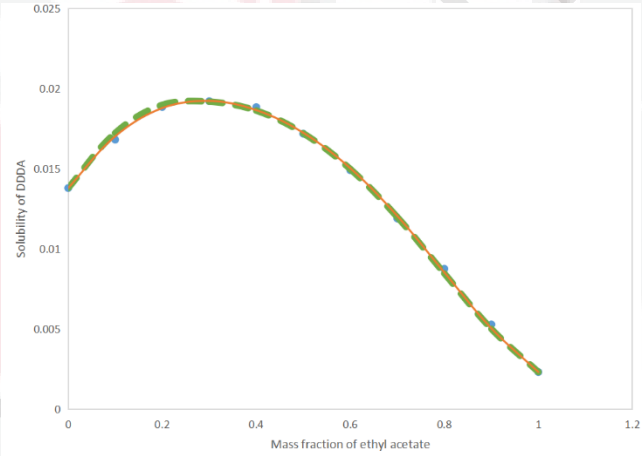

Figure S3 : solubility of DDDA (3) in ethyl acetate (1) + ethanol (2) cosolvent mixtures. Marker: experimental data; Solid line—: the model predicted values in the original article; Breaking line-----: modified Jouyban-Acree model

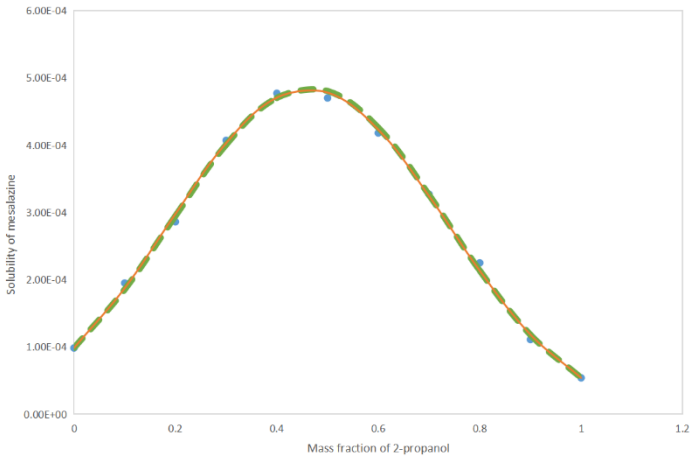

Figure S4 : Solubility of mesalazine (3) in 2-propanol (1) + water (2) cosolvent mixtures. Marker: experimental data; Solid line—: the model predicted values in the original article; Breaking line-----: modified Jouyban-Acree model

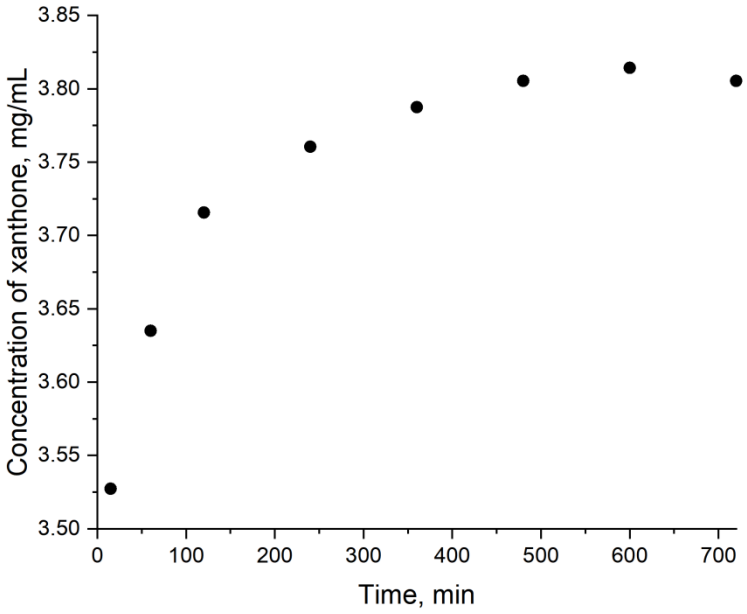

Figure S5 : Extraction cruve on extraction of xanthone from mangosteen pericarp by virgin coconut oil (VCO)+ethanol mixed-solvent (VCO volume fraction=0.6) with continuous stirring at 334.55K

The energy efficiency of an ultrasound horn was determined through calorimetric assessment of the actual energy dissipated using a documented method. Not all the energy generated by the sonicator during operation was transferred to the sample solution; only a portion was transferred from the probe tip to the medium. Amplitude percentages of 25%, 50%, and 75% were adjusted to calculate the actual power dissipated from the probe tip into the bulk of the medium by measuring the temperature rise of 100 mL water over

5 min. The actual power consumption values for the three different amplitude outputs measured in the experiment were 20.89 W, 44.06 W, and 63.35 W, respectively.

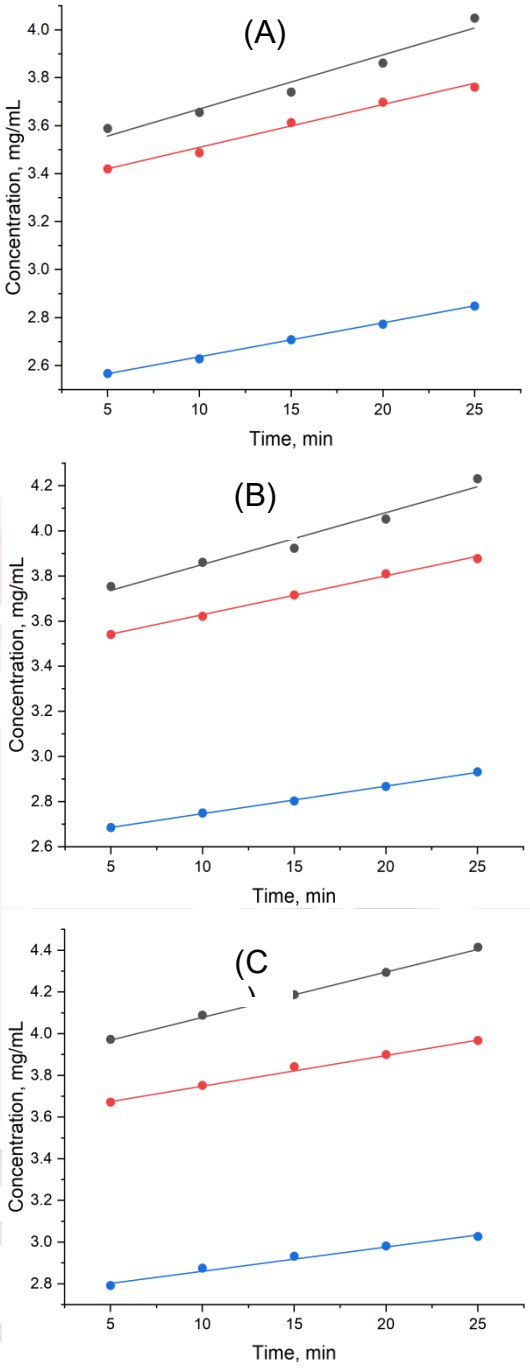

Figure S6 : Ultrasound-assisted extraction (UAE) was used to extract xanthone from mangosteen pericarp at ultrasound intensities of 17W(A), 21W(B) and 26W(C), respectively. The black, blue and red dots indicate a mixture of ethanol, virgin coconut oil (VCO) and mixed-solvent with VCO volume fractions of 0.6, respectively. The lines in the corresponding colors represent the fit results of the Peleg model

Regression Equation

Concentration = 2.467 + 0.02451 Time + 0.0646 Ultrasound intensity + 1.2721 Solvent ratio
+ 0.000099 Time*Time - 0.000396 Ultrasound intensity*Ultrasound intensity
- 1.8077 Solvent ratio*Solvent ratio - 0.000237 Time*Ultrasound intensity
- 0.00976 Time*Solvent ratio - 0.02274 Ultrasound intensity*Solvent ratio

Coefficients

Term	Coef	SE Coef	T-Value	P-Value	VIF
Constant	2.467	0.179	13.78	0.000	
Time	0.02451	0.00392	6.25	0.000	61.97
Ultrasound intensity	0.0646	0.0164	3.95	0.000	292.48
Solvent ratio	1.2721	0.0616	20.66	0.000	51.61
Time*Time	0.000099	0.000084	1.18	0.246	26.71
Ultrasound intensity*Ultrasound intensity	-0.000396	0.000374	-1.06	0.297	286.30
Solvent ratio*Solvent ratio	-1.8077	0.0313	-57.69	0.000	13.54
Time*Ultrasound intensity	-0.000237	0.000135	-1.75	0.088	39.07
Time*Solvent ratio	-0.00976	0.00121	-8.05	0.000	7.18
Ultrasound intensity*Solvent ratio	-0.02274	0.00233	-9.77	0.000	36.26

Model Summary

S	R-sq	R-sq(adj)	R-sq(pred)
0.0236269	99.85%	99.81%	99.74%

Analysis of Variance

Source	DF	Adj SS	Adj MS	F-Value	P-Value
Regression	9	12.5998	1.39997	2507.87	0.000
Time	1	0.0218	0.02181	39.07	0.000
Ultrasound intensity	1	0.0087	0.00869	15.57	0.000
Solvent ratio	1	0.2383	0.23828	426.85	0.000
Time*Time	1	0.0008	0.00078	1.39	0.246
Ultrasound intensity*Ultrasound intensity	1	0.0006	0.00062	1.12	0.297
Solvent ratio*Solvent ratio	1	1.8576	1.85758	3327.61	0.000
Time*Ultrasound intensity	1	0.0017	0.00172	3.07	0.088
Time*Solvent ratio	1	0.0362	0.03616	64.78	0.000
Ultrasound intensity*Solvent ratio	1	0.0533	0.05329	95.47	0.000
Error	35	0.0195	0.00056		
Total	44	12.6193			

Fits and Diagnostics for Unusual Observations

Obs	Concentration	Fit	Resid	Std Resid	
44	3.9668	4.0100	-0.0432	-2.13	R

R Large residual

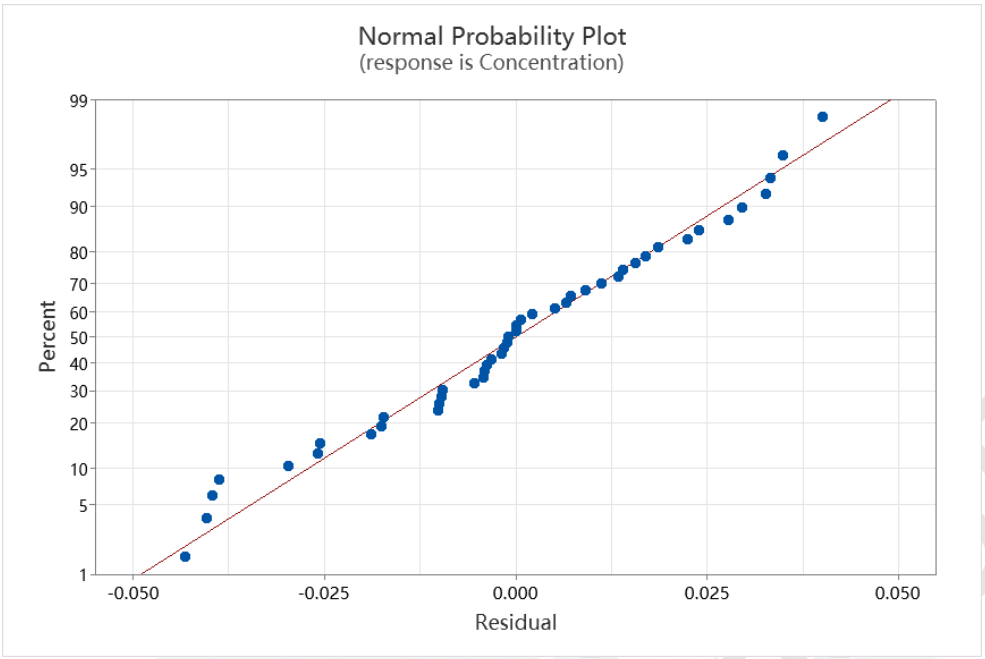

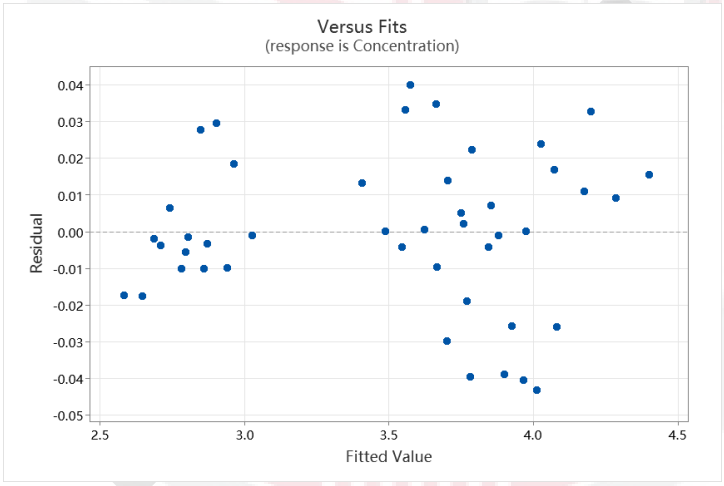

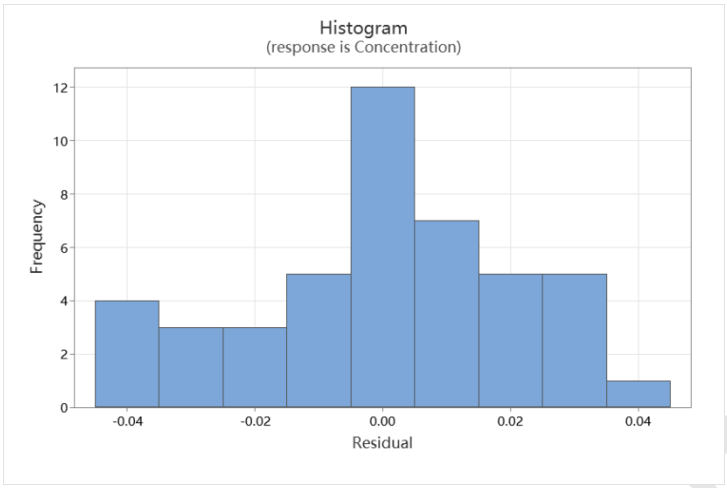

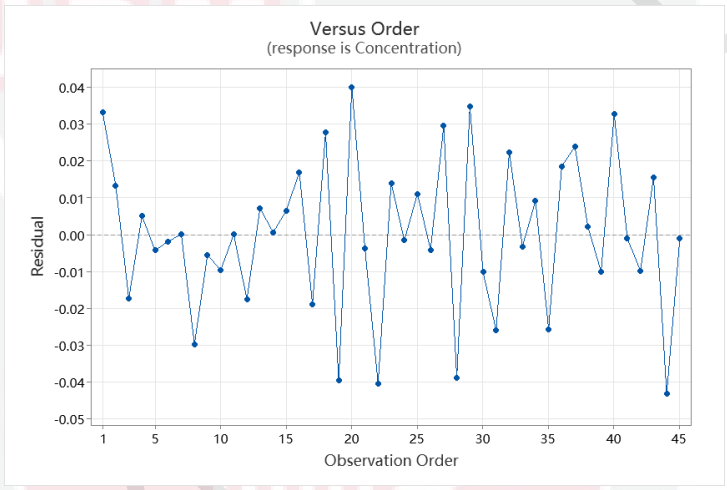

Figure S7 : Detailed statistics with response surface methodology showing ANOVA results for (a) extraction time, (b) ultrasound intensity, (c) solvent ratio

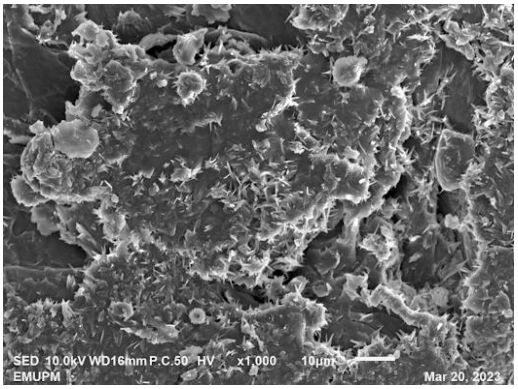

Powder 1 1000x

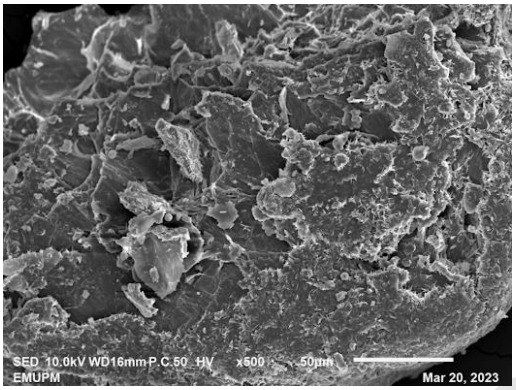

Powder 1 500x

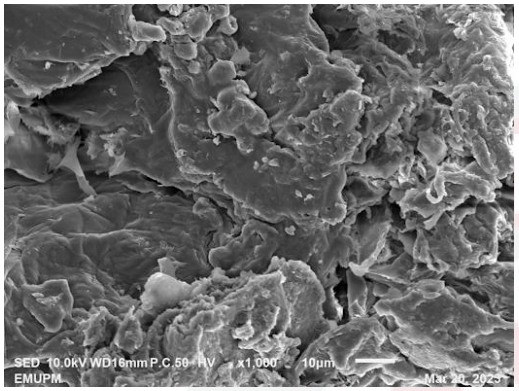

Powder 2 1000x

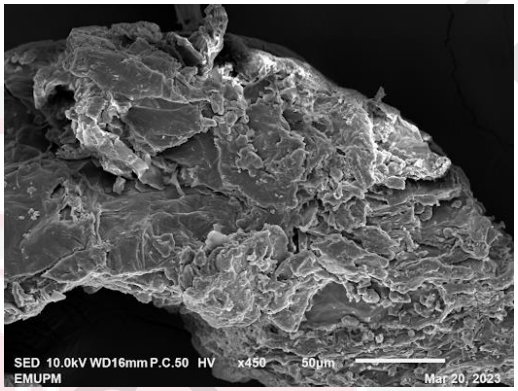

Powder 2 500x

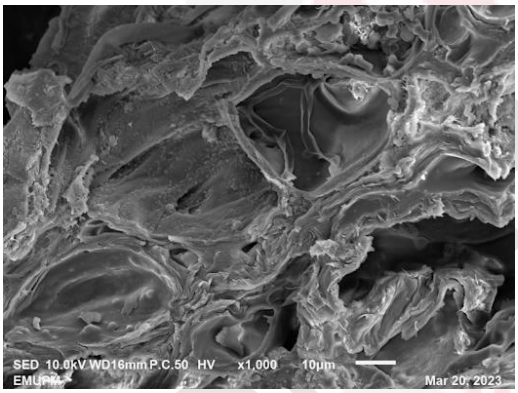

Powder 3 1000z

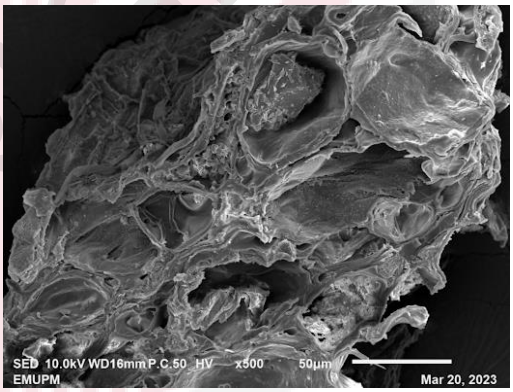

Powder 3 500x

Figure S8 : Scanning electron microscope (SEM) image of non-ultrasound- assisted extraction (UAE) mangosteen pericarp particles. Magnification is 500x and 1000x

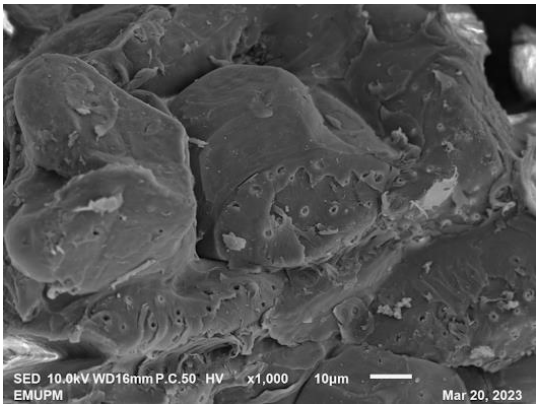

Powder 1 1000x

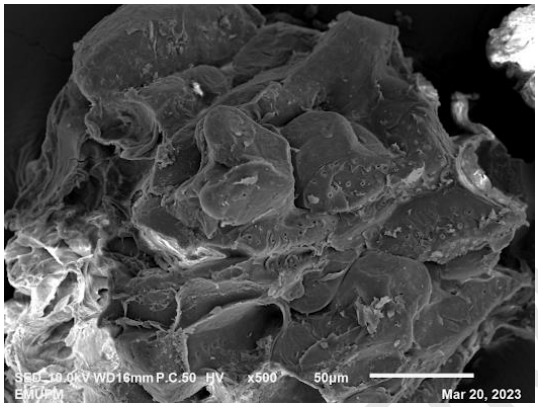

Powder 1 500x

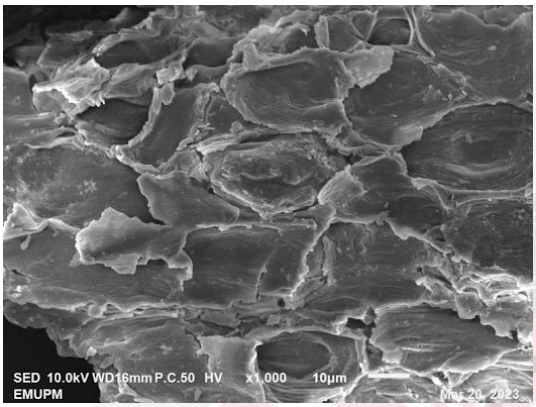

Powder 2 1000x

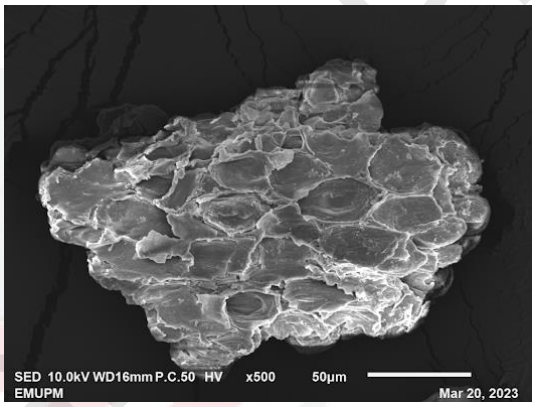

Powder 2 500x

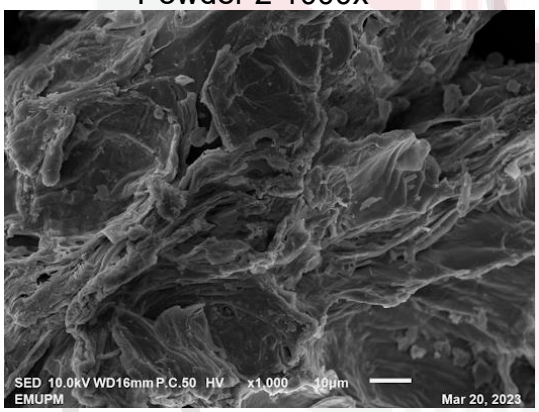

Powder 3 1000x

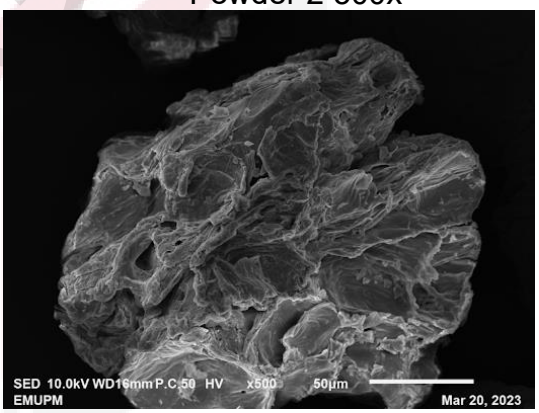

Powder 3 500x

Figure S9 : Scanning electron microscope (SEM) image of mangosteen pericarp particles after ultrasound- assisted extraction (UAE) processing with ethanol. Magnification is 500x and 1000x

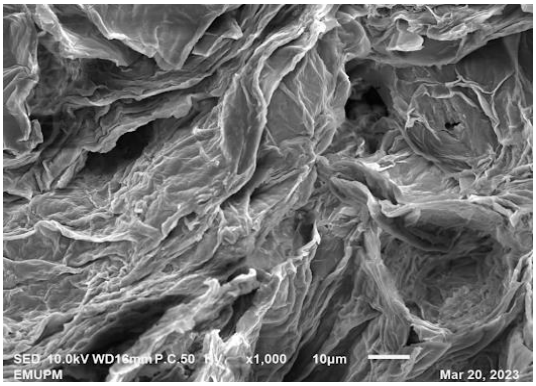

Powder 1 1000x

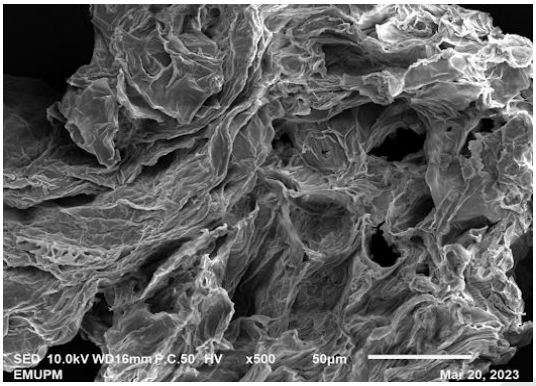

Powder 1 500x

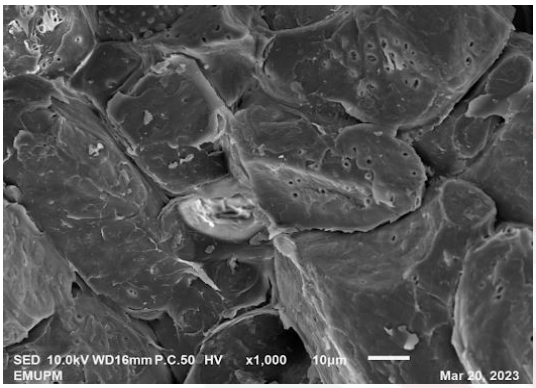

Powder 2 1000x

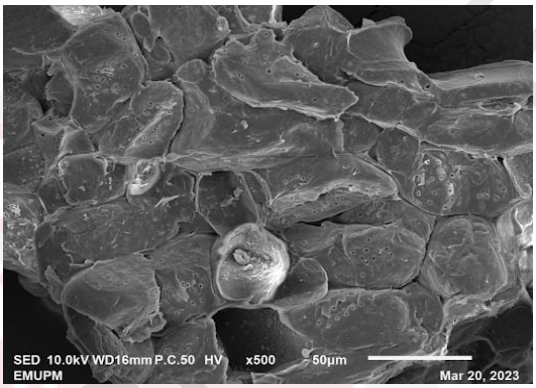

Powder 2 500x

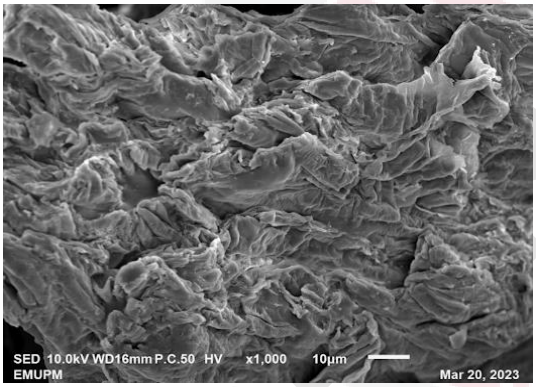

Powder 3 1000x

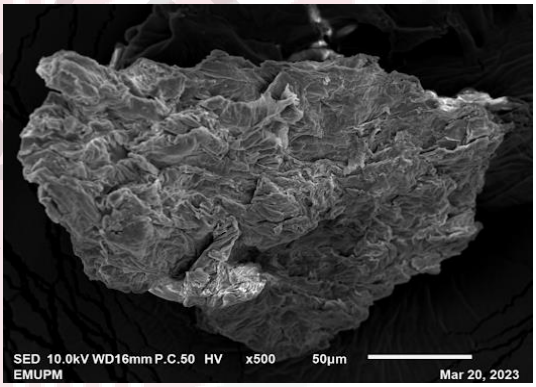

Powder 3 500x

Figure S10 : Scanning electron microscope (SEM) image of mangosteen pericarp particles after ultrasound- assisted extraction (UAE) processing with virgin coconut oil (VCO). Magnification is 500x and 1000x

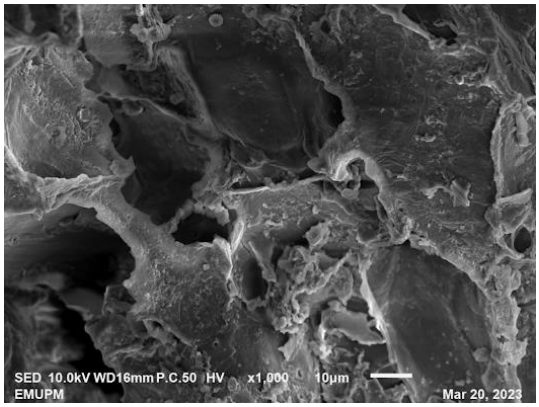

Powder 1 1000x

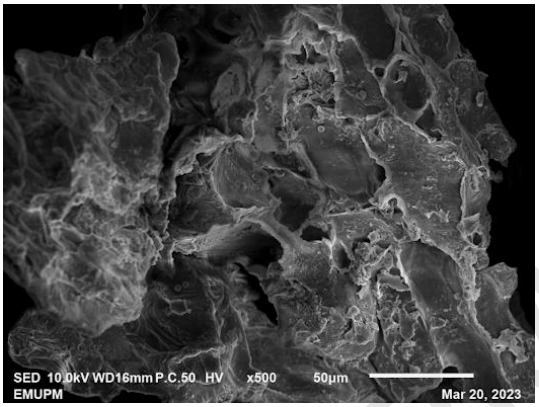

Powder 1 500x

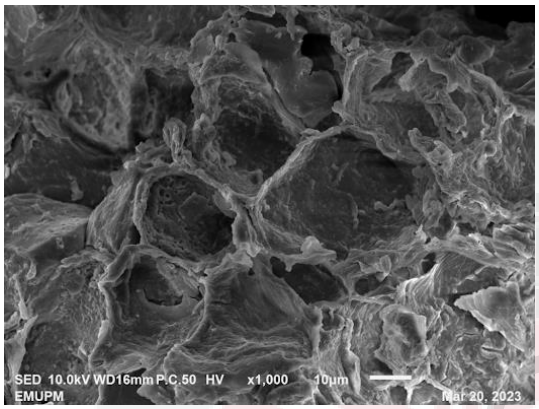

Powder 2 1000x

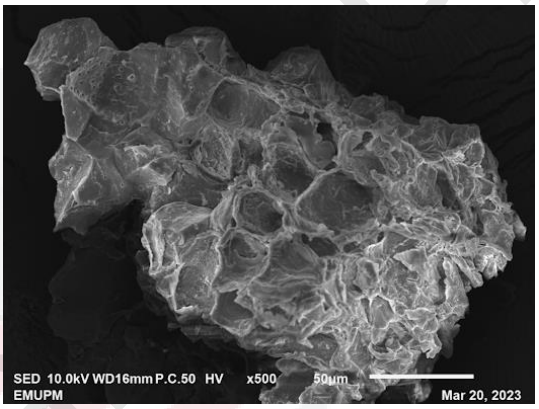

Powder 2 500x

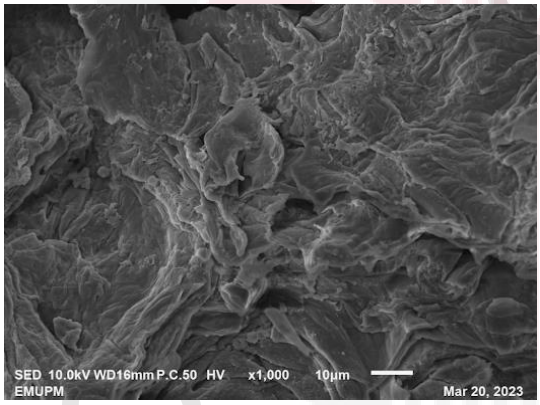

Powder 3 1000x

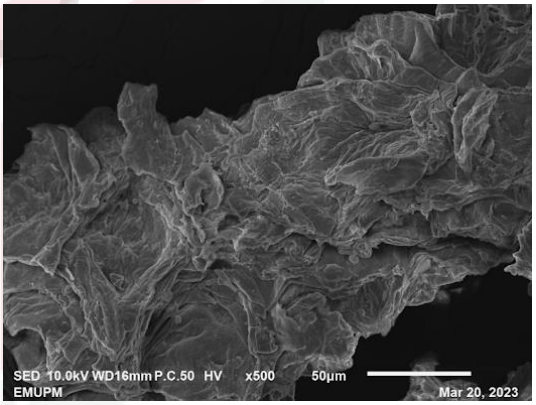

Powder 3 500x

Figure S11 : Scanning electron microscope (SEM) image of mangosteen pericarp particles after ultrasound- assisted extraction (UAE) processing with virgin coconut oil (VCO)+ ethanol mixed-solvent (VCO volume fraction=0.6). Magnification is 500x and 1000x

BIODATA OF STUDENT

Yao Zhengyuan (1996 -), male, born in Henan Province, China.

Obtained undergraduate degree in food science and technology from Henan University of Science and Technology, focusing on the design and stress analysis of tubular heat exchangers for the graduation project.

In college, he was engaged in deep processing of meat products and research and development of innovative meat fast food in Charoen Pokphand Foods.

Pursued postgraduate studies at Universiti Putra Malaysia, with a major in food technology. The research focused on the solubility model of xanthone in mixed solvents, extraction of active components from mangosteen peel, and ultrasonic-assisted extraction.

Concurrently, he participated in a joint training program with the Agro-Environmental Protection Institute, Ministry of Agriculture and Rural Affairs in China, where he conducted research on the green separation of lignocellulose and value-added transformation of separated products.

LIST OF PUBLICATIONS

Zhengyuan Yao. (2025). Synergistic effect of a VCO-ethanol solvent mixture and ultrasound-assisted extraction inenhancing xanthone extraction from mangosteen pericarp. Food and Bioproducts Processing, 150, 350-359.

Zhengyuan Yao. (2024). Deep Eutectic Solvent Pretreatment and Green Separation of Lignocellulose. Applied Sciences, 14 (17), 7662.